

Space Astronomy Instruments

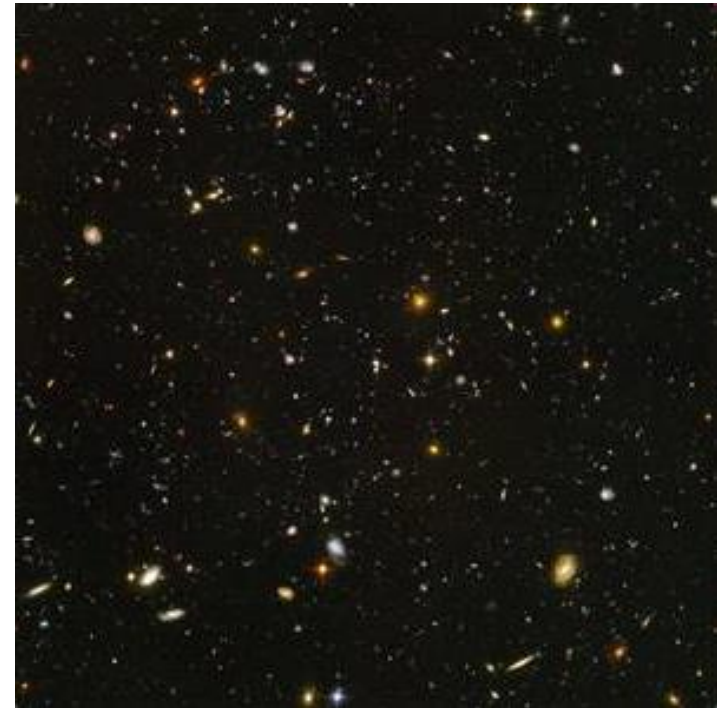
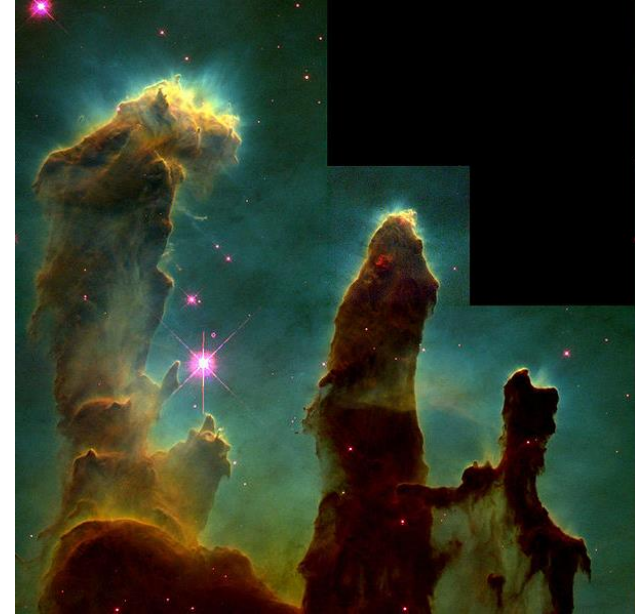
David Lumb, ESA Science Support
Office

Introduction

- **Some examples of instruments**
- **The special challenges especially cf. ground astronomy**
- **The environment and operations**
- **The engineering**

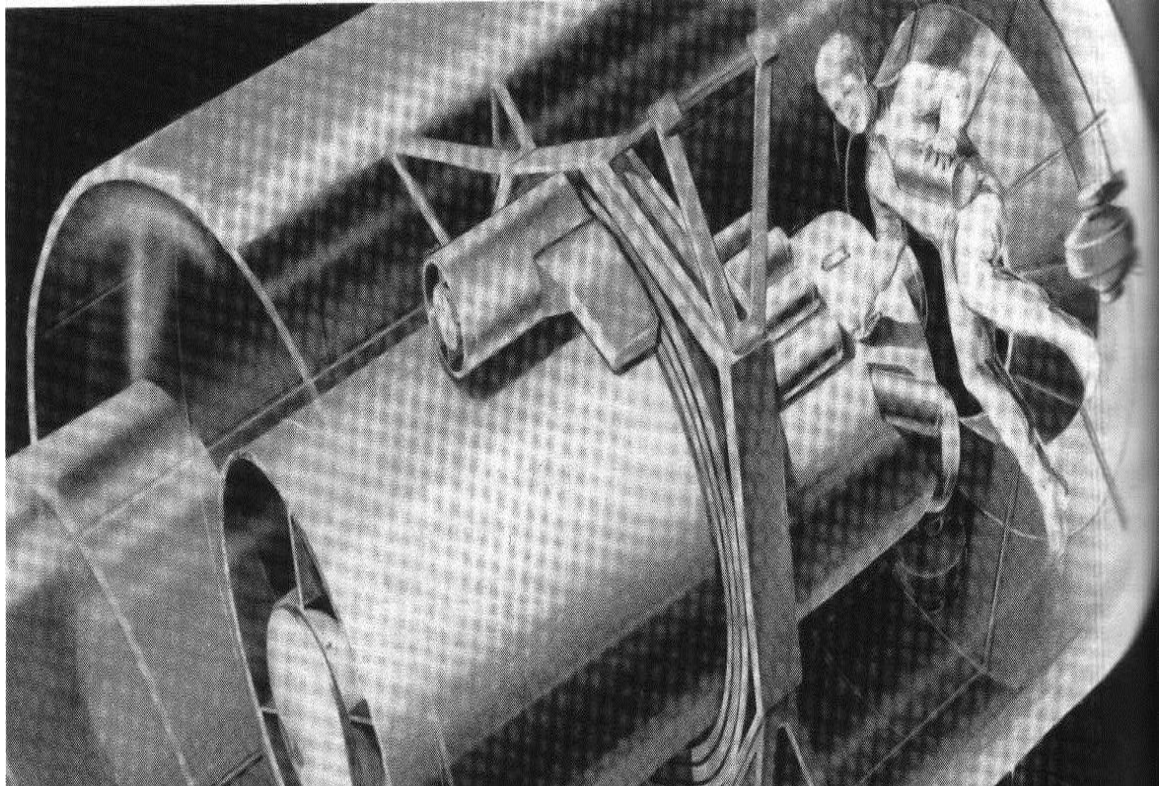
HST History

- Lyman Spitzer developed the concept of a telescope in space. In 1946 — more than a decade before the launch of the first satellite
- In 1962, the USA's National Academy of Sciences recommends building a large space telescope.
- In 1977, Congress votes to fund the project and construction of Hubble Space Telescope begins.
- Launch in 1990 — discovery of the spherical aberration
- 1993 — first Servicing Mission
- 1995 — first Hubble Deep Field data



Early Instrument Concepts

- Earliest concepts considered astronauts periodically retrieving film!



CCDs eventually prevailed over vidicons after a period of “*invention push & market pull*” driven by NASA and CCD manufacturers

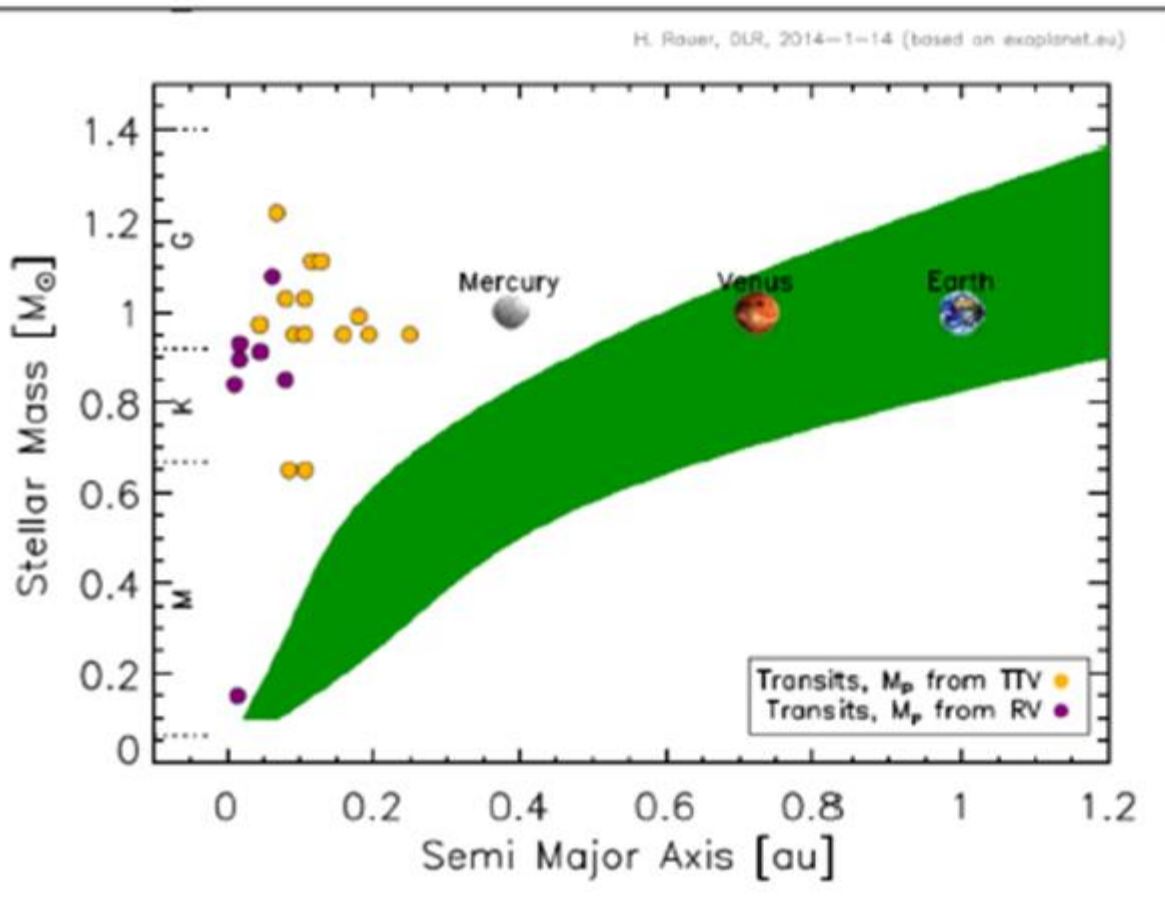
Space vs Ground

- **Seeing / Absorption / Scattering**
- **Resolution advantage of HST over ground-based telescopes has been decreasing as adaptive optics systems become more widespread.**
- **One advantage of the larger ground-based telescopes is their sensitivity as their primary mirrors are much larger.**
- **Space-based telescopes essential for most IR, UV, X-ray and γ -ray observations. Developments over decades have seen improvements in resolution, sensitivity and operational life spans.**

Exo-Planets from space

- **Detection of a large number of exoplanets and the detailed analysis of their central stars, including seismic analysis.**
- **Achievable by a very high precision, very long duration and high duty cycle photometric monitoring from space of a very large sample of stars.**
- **The Earth's atmosphere disturbances limit the achievable performance to millimag accuracies, mostly through scintillation noise. The small amplitude of the photometric dips caused by terrestrial planets are therefore beyond the range of ground-based observations.**
- **Long, uninterrupted observations, that only space-based instruments can provide, are necessary to optimize the probability of transit detection, and to see several successive transits in order to measure the orbital period,**

“Super-Earths” characterised with Radius and Mass

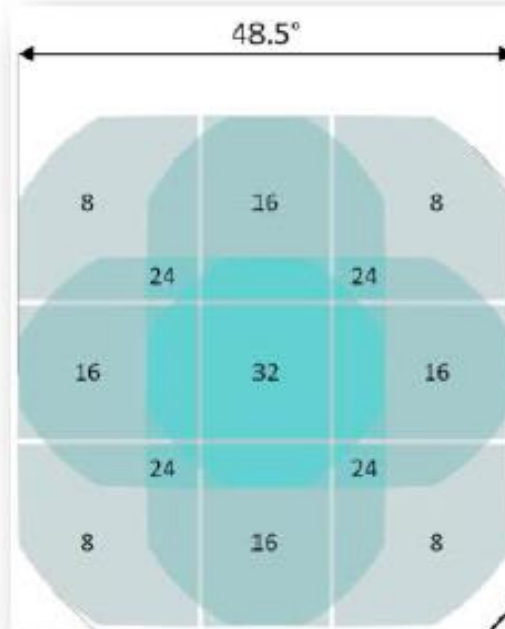
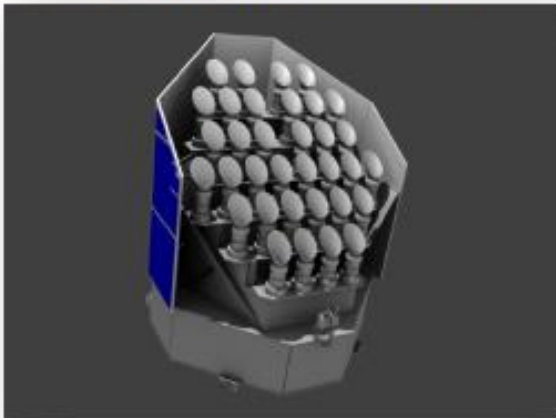


- Goal: Detect and characterize super-Earths in habitable zones
- Status: very few small/light planets in habitable zones detected

→ No characterized „super-Earths“ in its habitable zone

Multiple telescopes + CCDs

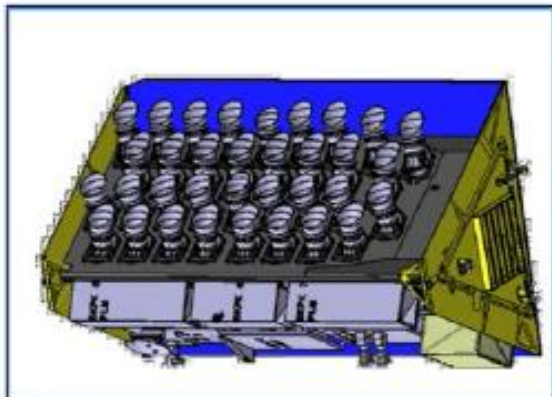
Two designs studied:



Multi-telescope approach:

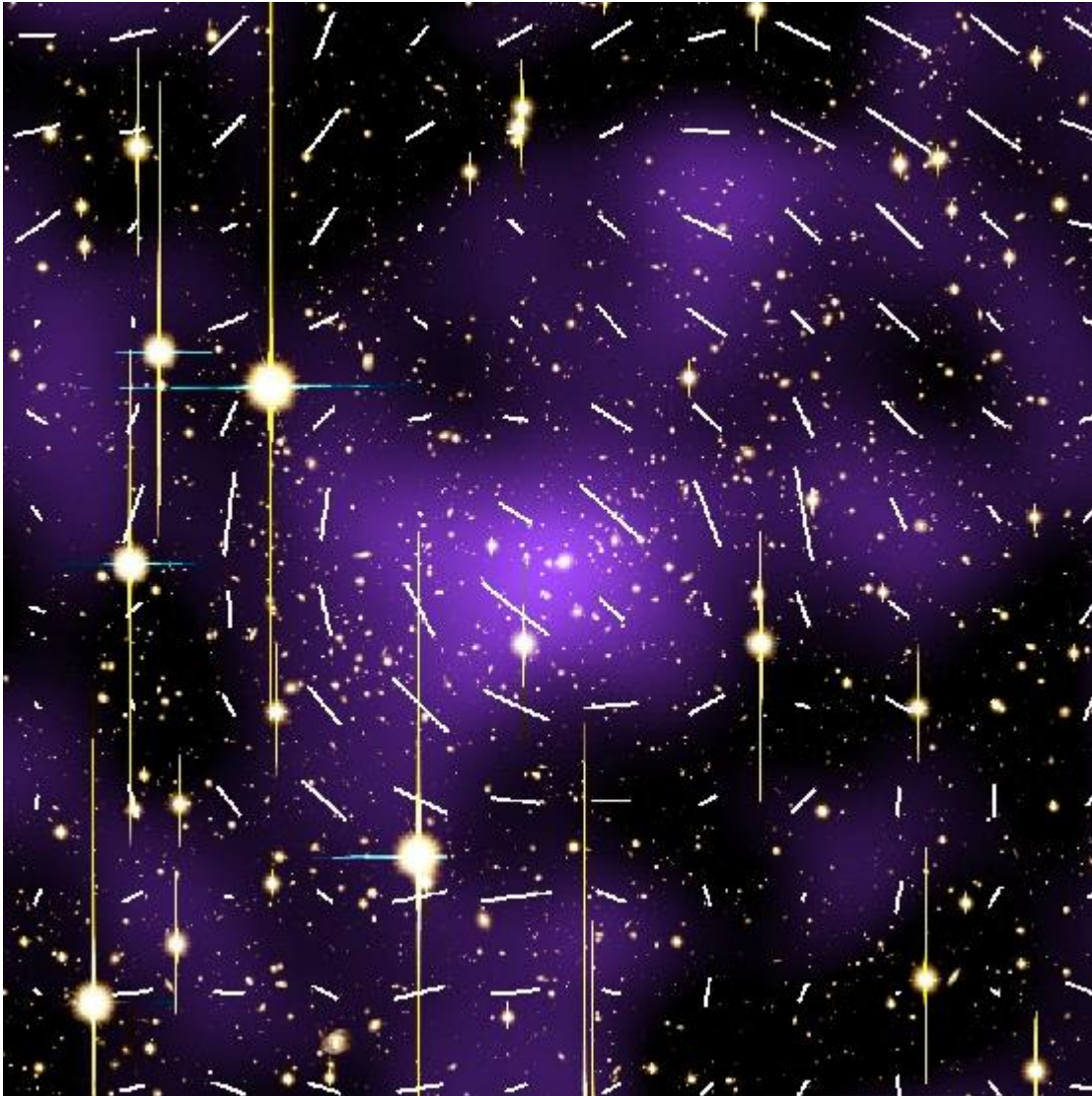
- *Large FOV (Large number of bright stars)*
- *Large total collecting area (provides high sensitivity allowing asteroseismology)*
- Redundancy

- Cameras are in groups
- Offset to increase FoV



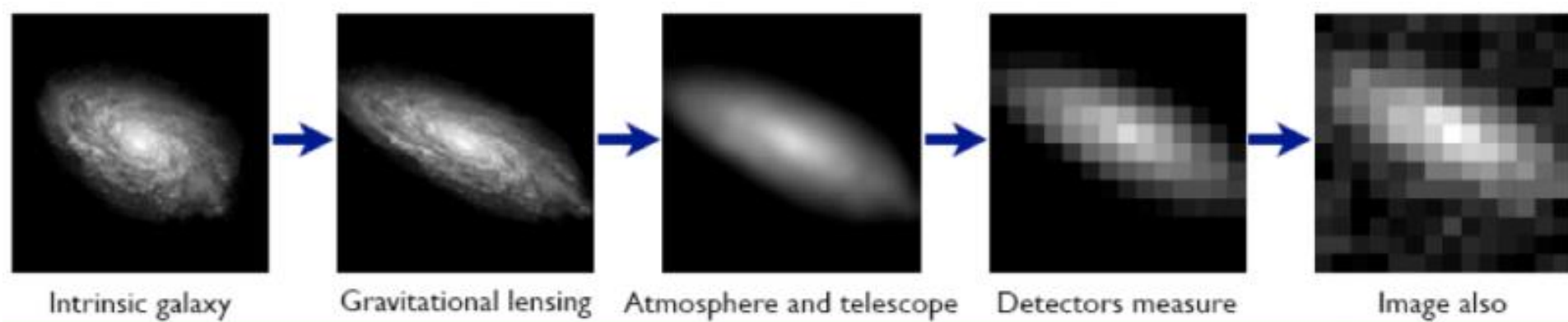
- 32 «normal» 12cm cameras, cadence 25 s, white light
- 2 «fast» 12cm cameras, cadence 2.5 s, 2 colours
- dynamical range: $4 \leq m_V \leq 16$
- L2 orbit
- Nominal mission duration: 6 years
- Field-of-View: $48.5^\circ \times 48.5^\circ$ (2250 square degrees)

Weak Lensing



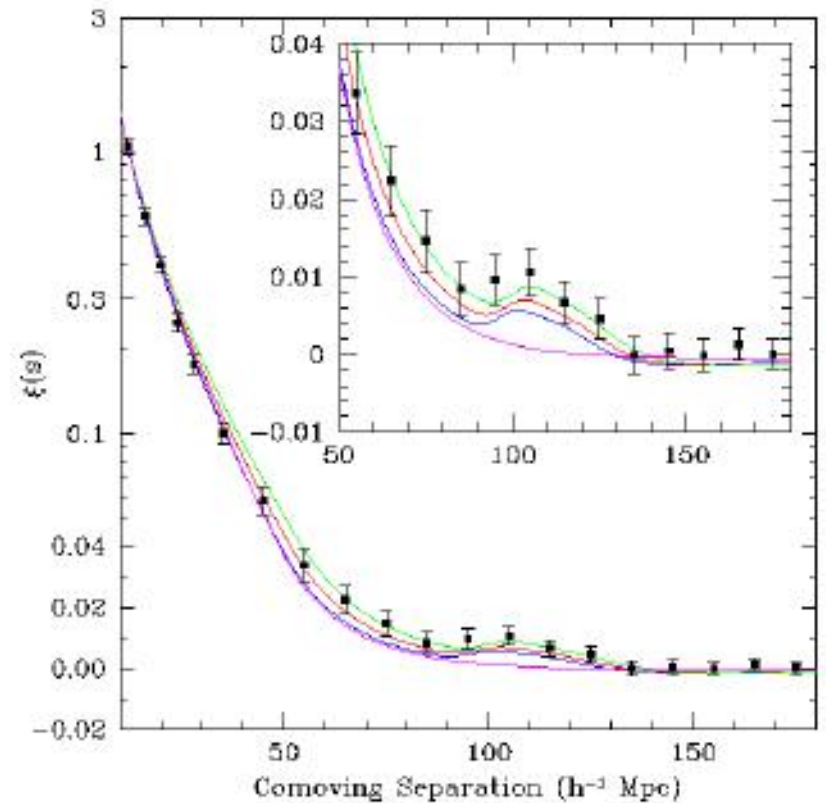
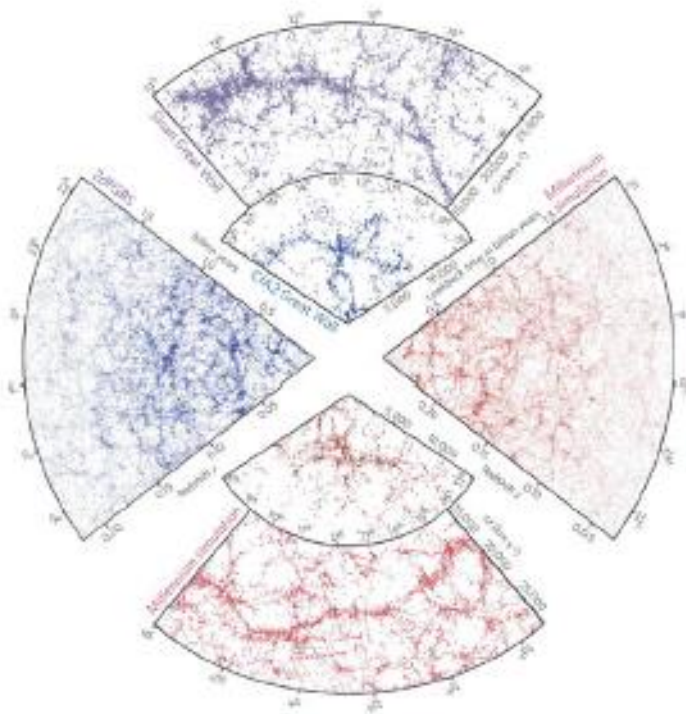
- Systematic alignment of background sources
- Integrated effect of all luminous and dark matter

Weak Lensing



- Eculid Mission offers advantage from space for removal atmosphere effects
- L2 orbit location allows very stable thermal environment, so that the telescope PSF is not variable with time

BAO



(Left panel) The galaxy distribution in the largest surveys of the local Universe, compared to simulated distributions from the Millennium Run
 (Right panel) The two-point correlation function of SDSS “luminous red galaxies”, in which the BAO peak at $\sim 105 h^{-1} \text{ Mpc}$ has been clearly detected

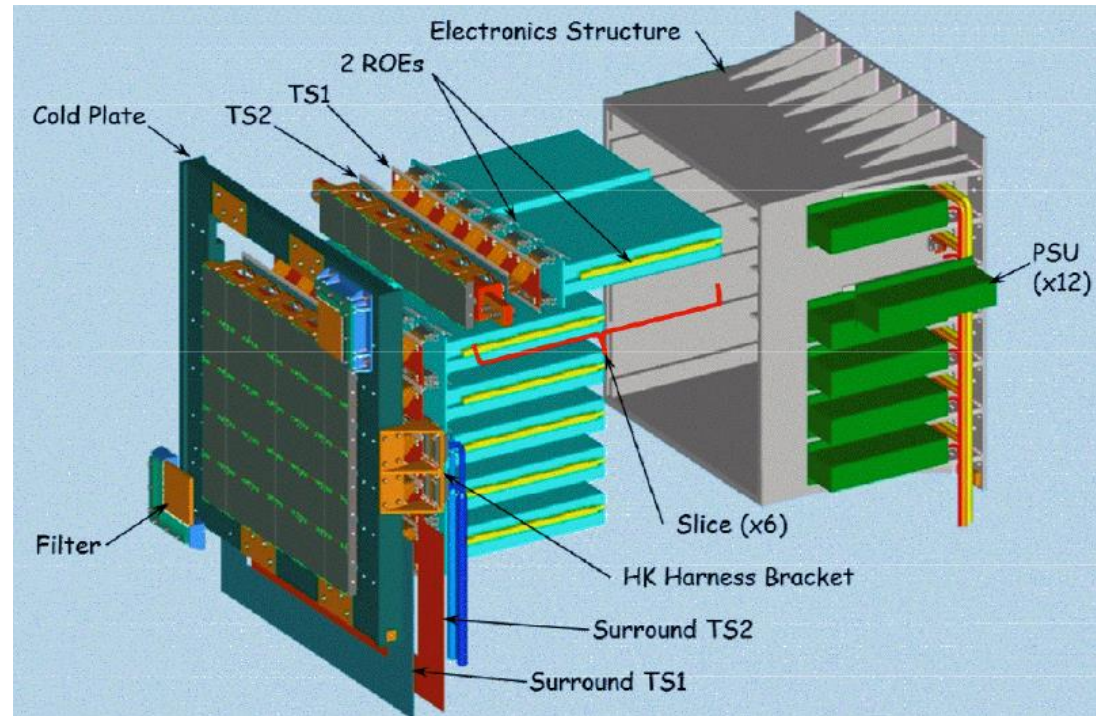
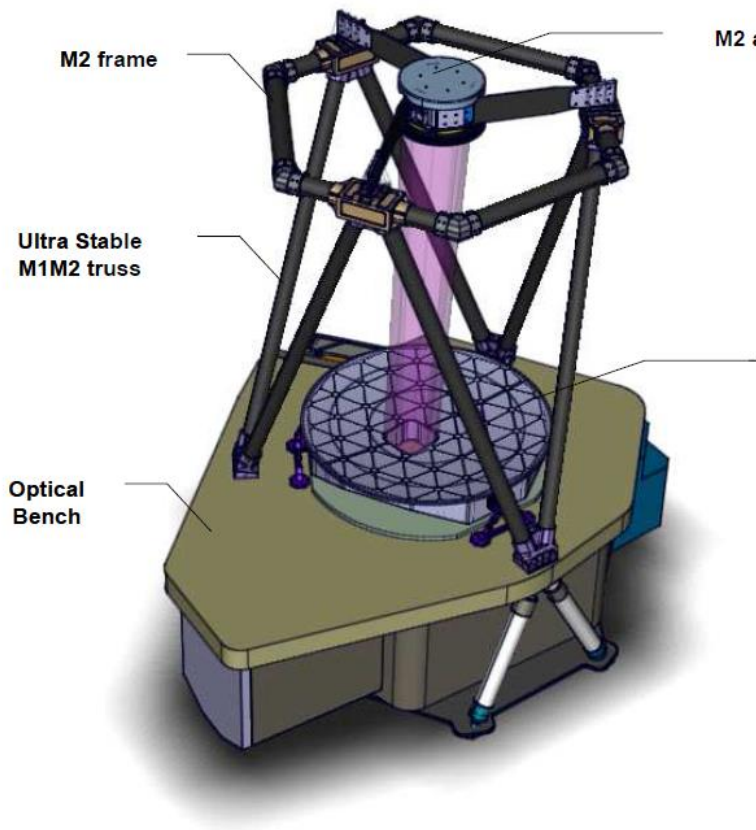
A package of measurements

- **A small and stable PSF:** The cosmic shear survey requires accurate measurements of the shapes of many galaxies - possible thanks to the stability & exquisite image quality of Euclid . Minimises any corrections for the inevitable blurring caused by the PSF. *Stability allows the PSF to be known accurately as a function of time and across the field of view.*
- **Deep NIR photometry:** Weak lensing tomography also requires redshifts of the source galaxies. Euclid will obtain *photometric redshifts* from multiband photometry. Needs small scatter and outlier rate - NIR observations are required. Done from space because of the much lower background. Euclid will therefore provide NIR photometry which is *three magnitudes deeper* than can be achieved from the ground over such a large area.

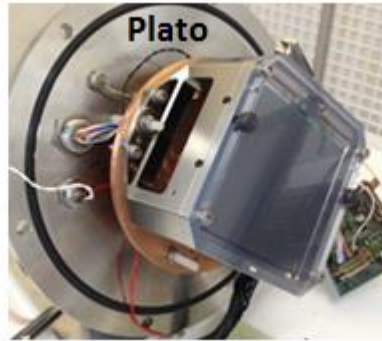
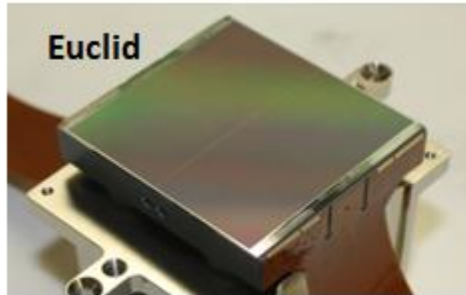
A package of measurements

- **Deep NIR spectroscopy:** The precision measurements of the clustering of galaxies require an unprecedented number of redshifts for galaxies over most of the extra-galactic sky in the redshift range $0.7 < z < 2.1$ in order to probe the epoch when dark energy became important. This requires measuring the **H α line using deep NIR spectroscopy** that can only be provided by space observations,
- *the resulting data-set homogeneous, uniform and well-controlled on large-scales, which is fundamental to minimise the sources of potential **systematic error***
- *it possible to perform a survey of 15,000 deg² extended to $z \geq 2$ in ≤ 6 years, including both imaging and spectroscopic observations.*

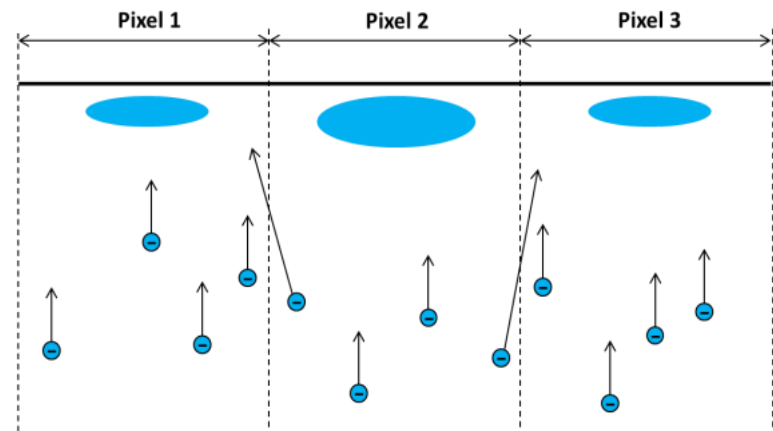
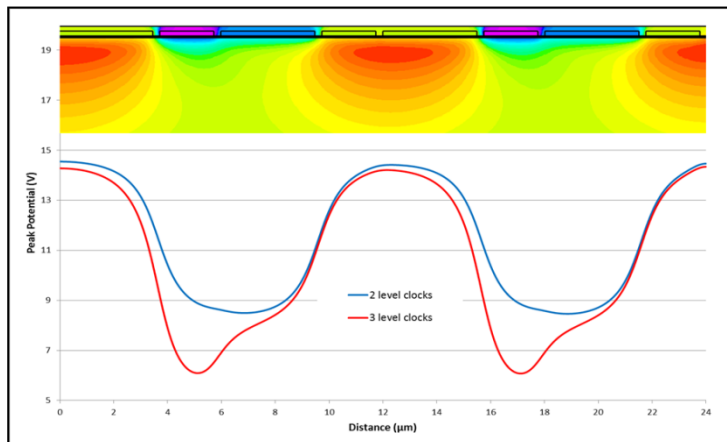
Thermal stability



CCDs and Precision



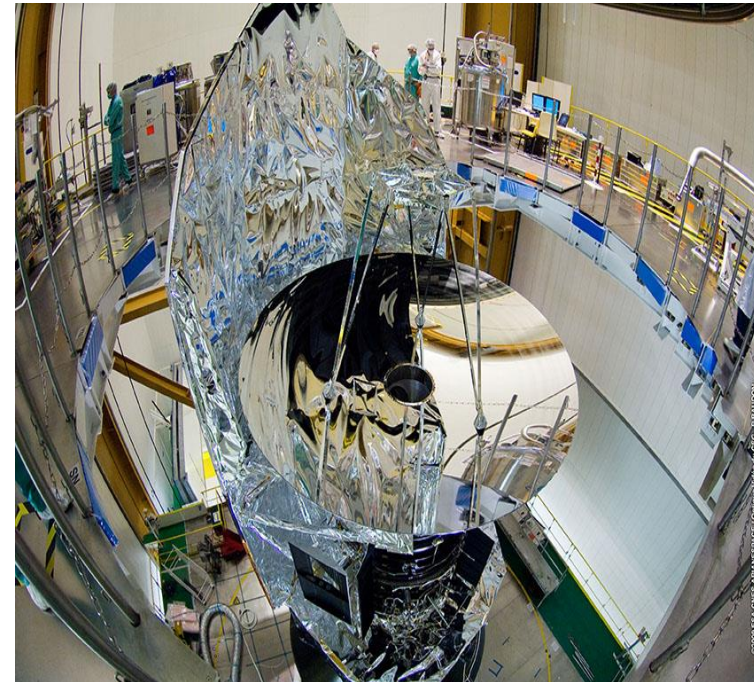
- Radiation damage – smears out PSF, removes signal charge (p channel, clocking sequences)
- Signal-dependent charge re-distribution can lead to distortions in PSF shapes which also need calibration



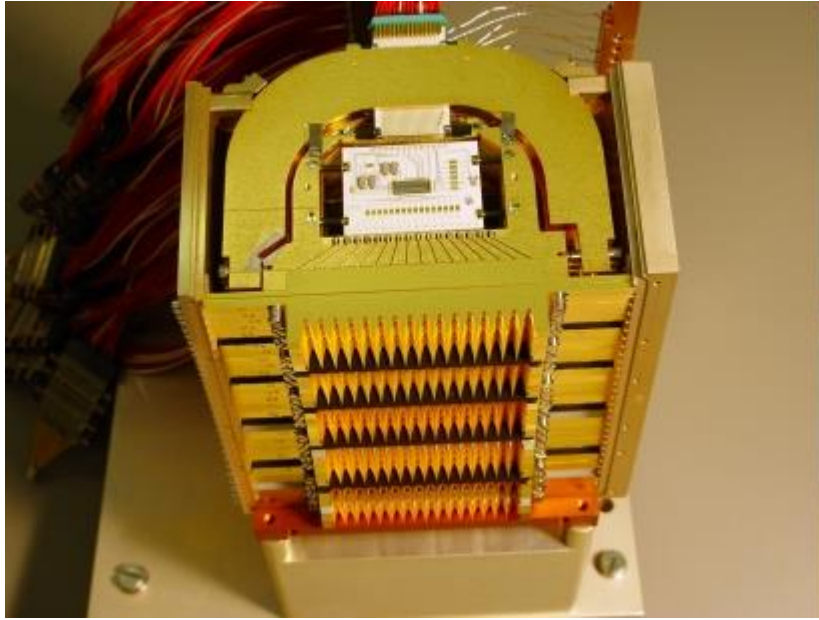
Herschel Instruments

- **PACS is a camera and low to medium resolution spectrometer** in range 55-210 μm . Four detector arrays, two bolometer arrays and two Ge:Ga photoconductor arrays. The bolometer arrays for wideband photometry. Photoconductor arrays are exclusively for spectroscopy. PACS operated either as an imaging photometer, or as an integral field line spectrometer.
- **SPIRE is a camera and low to medium resolution spectrometer** Wavelengths in the range 194-672 μm . An imaging photometer and a Fourier Transform Spectrometer (FTS), use bolometer detector arrays.
- **HIFI is a very high resolution heterodyne spectrometer** covering the 490-1250 GHz and 1410-1910 GHz bands. Low noise detection using superconductor-insulator-superconductor (SIS) and hot electron bolometer (HEB) mixers, together with acousto-optical and autocorrelation spectrometers. HIFI is not an imaging instrument, it observes a single pixel on the sky at a time.

3.5 m diameter silicon carbide mirror



PACS



- **Ge:Ga photoconductor** - application of stress shifts the cut-off wavelength to higher values by breaking the degenerate valence band forcing the heavy hole band closer to the acceptor state thus allowing less energetic photons to excite free charge carriers
- *Responsivity changes to irradiation!*



- **Top**

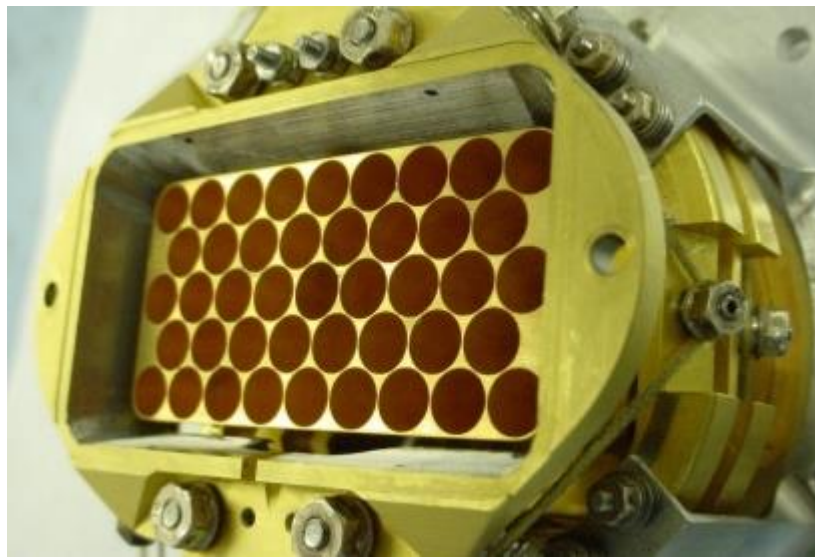
Scanning electron microscope (SEM) micrograph of part of one PACS 16 × 16 bolometer matrix.

- **Bottom**

The detail, marked by the red rectangle, shows the structure of one pixel: a (coarser) grid in the front acts as a resonant absorber while the (finer) grid in the back acts as a $\lambda/4$ back-reflector.

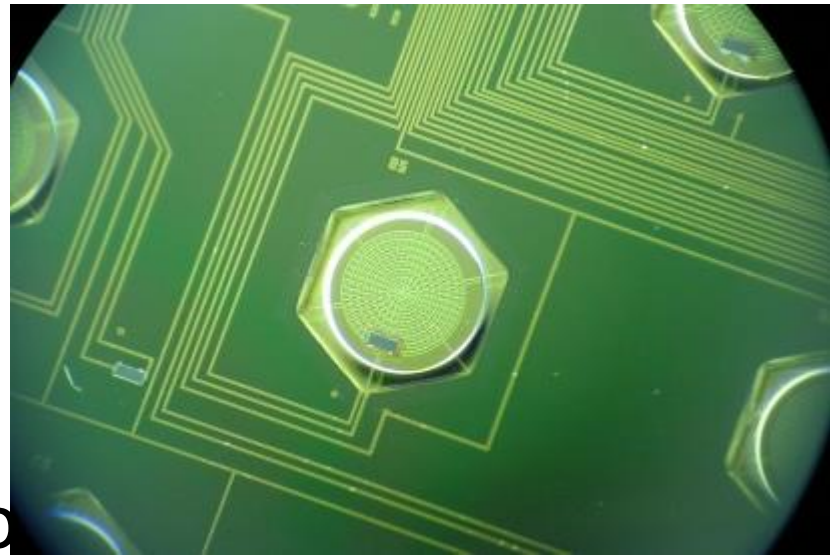
SPIRE

- The SPIRE photometer has three arrays of bolometer detectors each dedicated to one of the instrument's three wavelength bands centred on approximately 250, 350 and 500 μm . This image shows the whole detector assembly for the 500 μm band. The 43 holes in this front view of the assembly are the entrances to feedhorns that direct the light onto the actual detectors: 43 bolometers lying behind the feedhorns in the assembly.



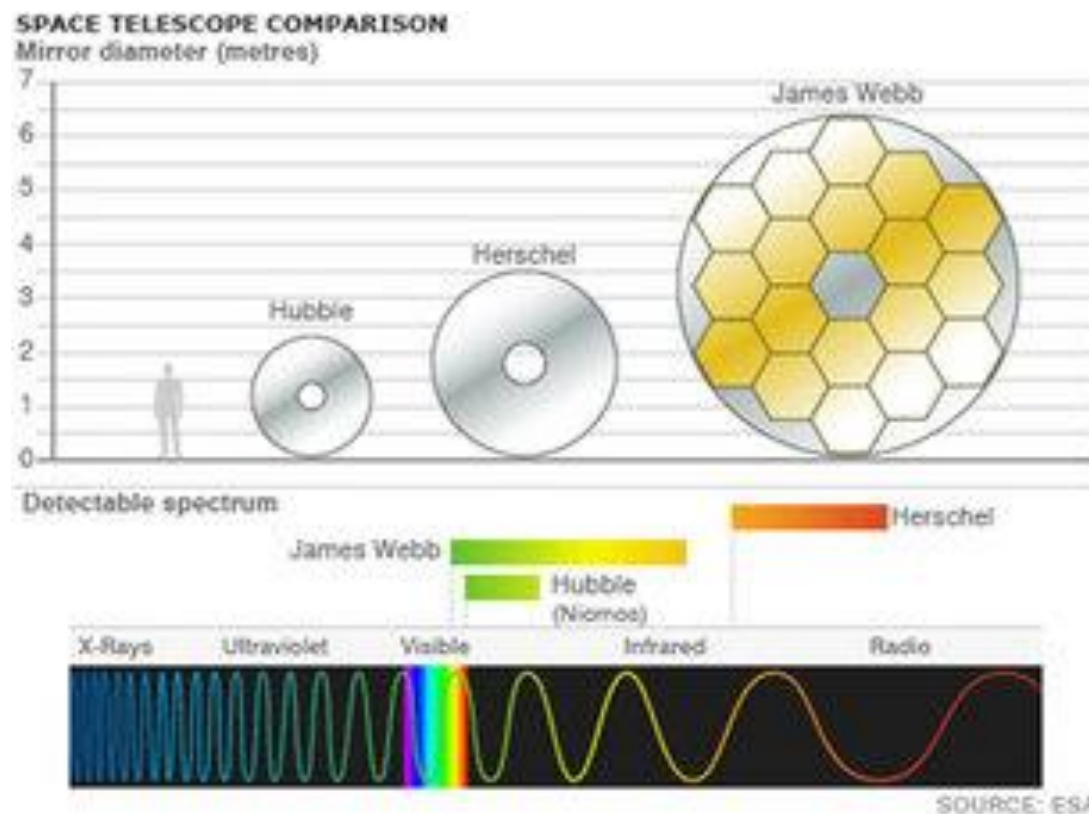
SPIRE

- Close-up of a single bolometer, hexagonal in shape, with parts of surrounding bolometers also visible.
- The tiny crystal (towards the bottom of the bolometer), reacts to changes in temperature. When a source on the sky is observed, the green circular area of the bolometer absorbs the energy from the light that falls on it and heats up by a small amount.
- Measurement of brightness is carried out by measuring crystal the change in resistance



Herschel Telescope

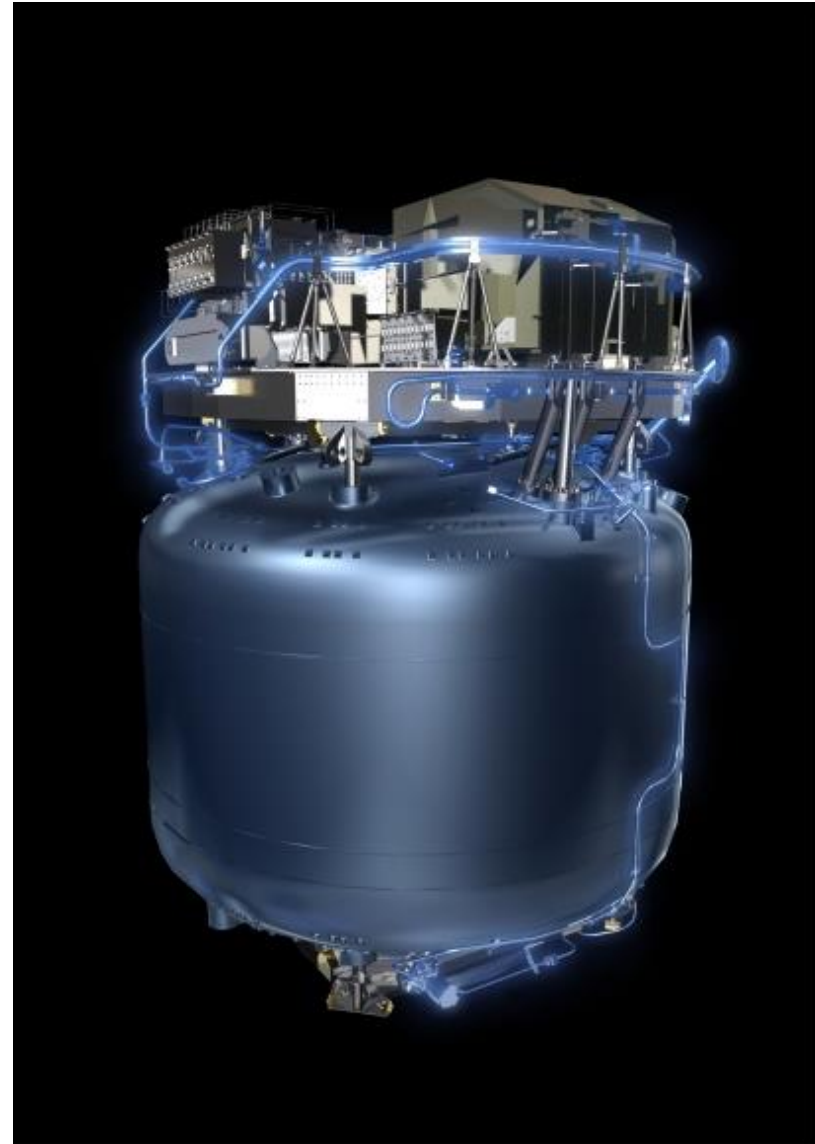
- The Herschel mirror was constructed of silicon carbide. The primary mirror was made out of 12 segments brazed together to form a monolithic mirror



Machined and polished to the required thickness (about **3 mm**), shape, and surface accuracy. (**1 micron**)

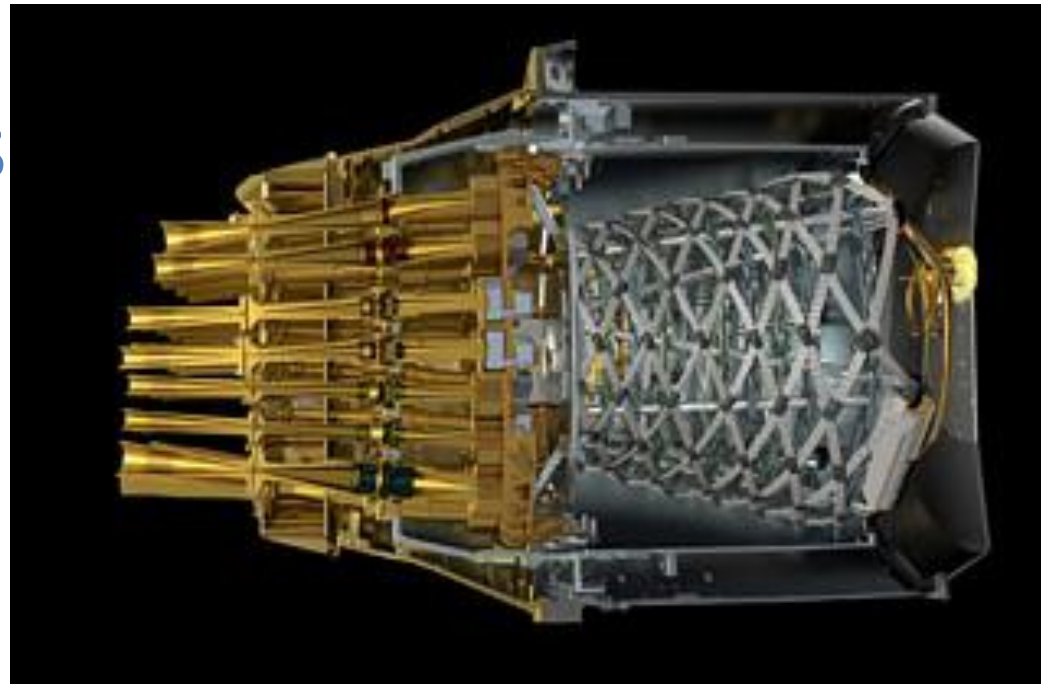
Herschel Cryostat

- Large cryostat maintaining instrument temperature of 1.7 K for 4 years. Helium-II conditions by vacuum pumping for several days to below the Lambda point at about 2.17 Kelvin then lowered even further by continued vacuum pumping to about 1.7 Kelvin.
- Continually refilled with He & pumping until four days before the launch
- After the launcher fairing placed over the Herschel and Planck spacecraft, access points used to ensure the cryostat tank itself is kept as cold as possible for the following days by flushing helium gas
- The helium is used to cool the three science instruments' focal plane units (FPU) and the shields.
- Porous plug allows separation of the gas from the boiling liquid helium such that only gas leaves the tank. It slowly flows from the tank into pipes around the payload (highlighted in blue) to cool it to between 1.7 K, 4 K and about 10 K.



Planck Instruments

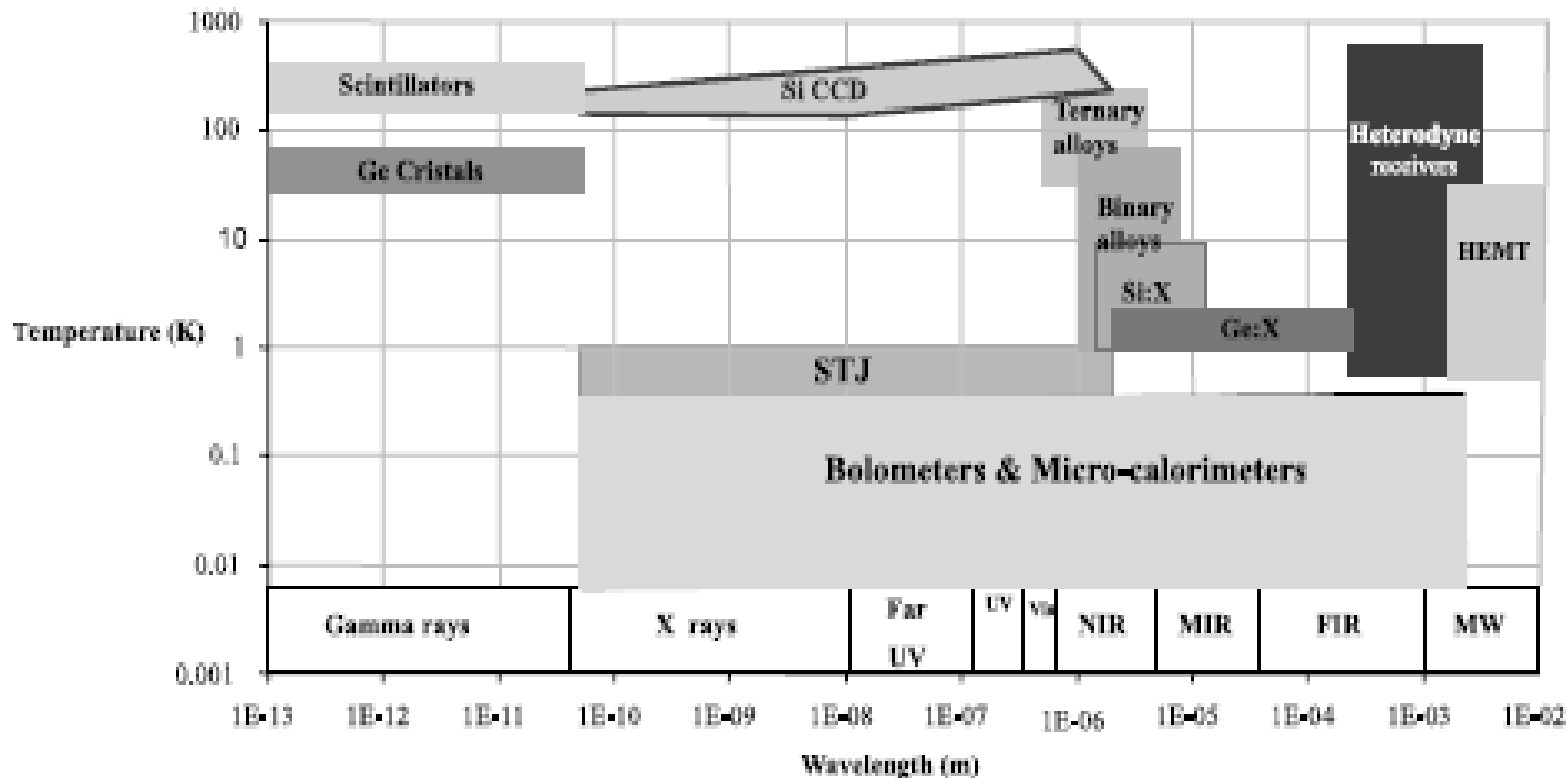
- Planck's Low Frequency Instrument (LFI), and the High Frequency Instrument (HFI), are equipped with a total of 74 detectors covering nine frequency channels.
- 3-stage refrigeration chain which takes over after the passive cooling system ~ 50 K. Dilution refrigerator 0.1K



Sensors and cooling

Cryogenic photon detectors offer advantages in terms of

1. *Higher sensitivity in terms of NEP*
2. *Better energy resolution $E / \Delta E = \lambda / \Delta \lambda$*



System Design Issues

- Decision to adopt cryogenic design will be based on trade-off analysis considering among others the mass savings, power consumption and reliability
- Total energy balance depends critically on the efficiency of the system:
- Passively cooled subsystem has positive energy balance, while actively cooled (eg Stirling cooler) has a critical energy balance
- Choice between passively and actively cooled design depends on operating temperature and even the type of orbit of the satellite

Cooler Systems

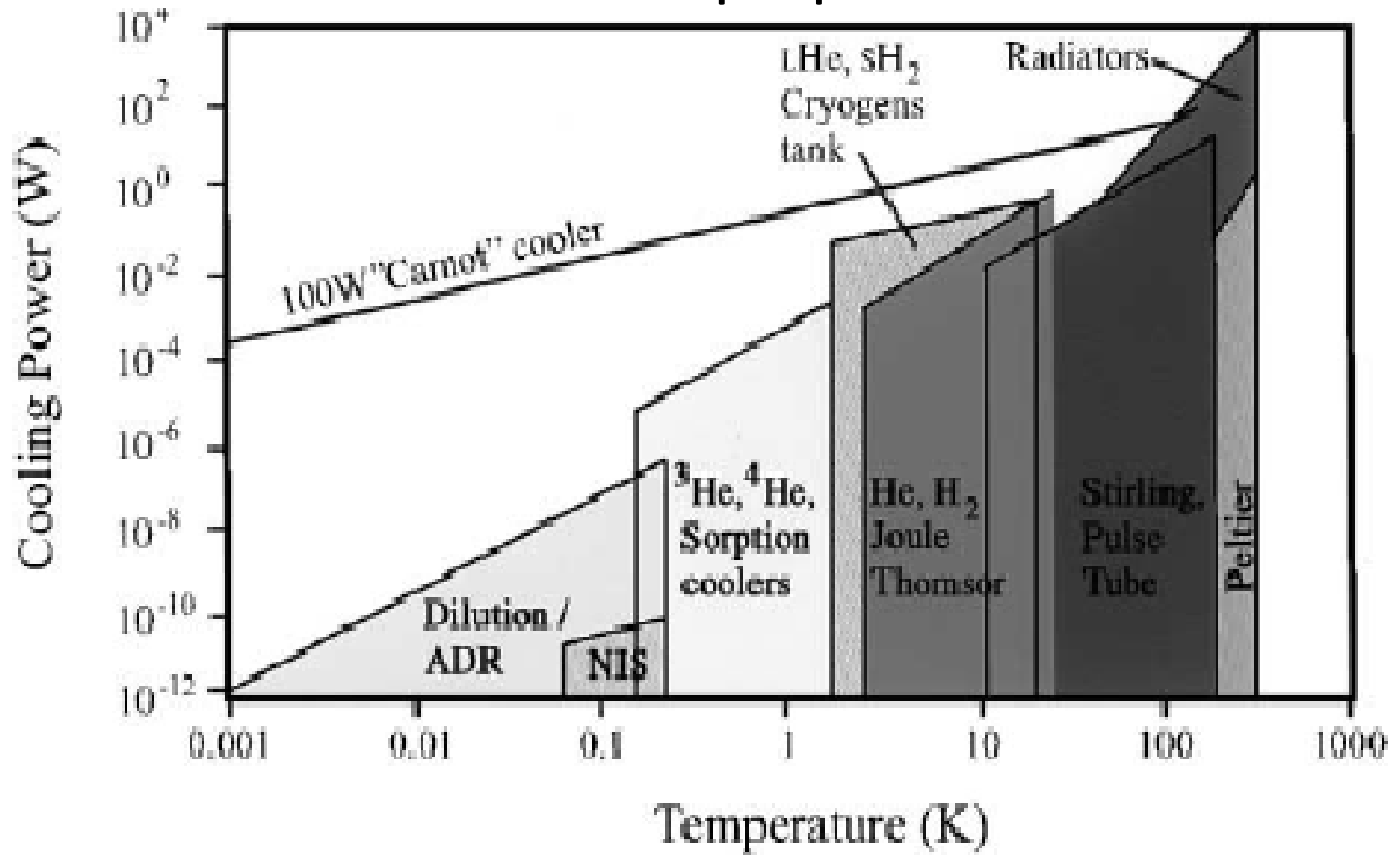
- Cooler must have heat lift compatible with satellite size and power resources
- Low temperature equipment must be properly supported, insulated from the room temperature satellite bus & protected from solar/earth radiation
- Cold parts have to be accessed for wiring and for the optical input
- Ancillary equipment has also to be cooled (heat links, heat switches, filters thermometers)
- Testability of the system (instrument performance, environment qualification tests) has to be ensured

Engineering for space

- Cooling system must survive vibrations of launch (compromise between cross-section for support and for thermal isolation)
- Cooler must operate in zero gravity for period time ~years
- Payload needs to be built from materials compatible for both space and cryogenic environment
- No vibrations or pick-up sensitive elements
- Lifetime (MTBF) of equipment should be compatible with and exceed nominal mission duration and operational cycles (ECCS Standards !)

Types of cooler

- Passive radiator to deep space 2.73K

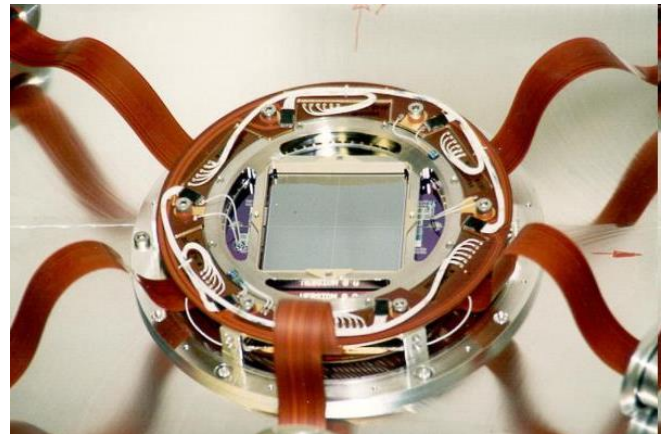
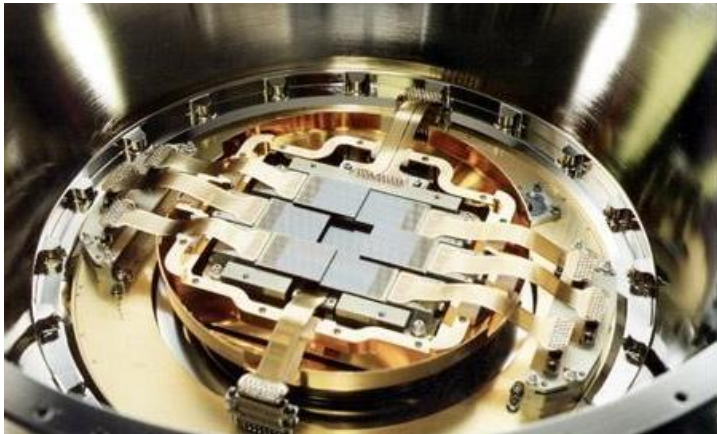


Bolometers for High Energy

- Not immediately apparent this technology would be applicable:
- The total energy deposited by X-rays from the sky via focussing telescopes over 30-40 years of observatories would heat a teaspoon of water ~ 1 microKelvin
- To date relied on \sim conventional CCDs

CCDs for X-ray

- Essentially the same operation as for visible band, except read out fast enough to guarantee single photon counting
- Energy absorbed and photoelectron cascade liberates 1 e/h pair per 3.65eV
- $\Delta E_{(fwhm)} = 2.35 * \sqrt{(r^2 + \frac{F^E}{3.65})} \sim 100\text{eV}$
- Broad band temperature diagnostics – calibration? (Planck cosmology depends on XMM cluster temperatures)



X-ray Optics

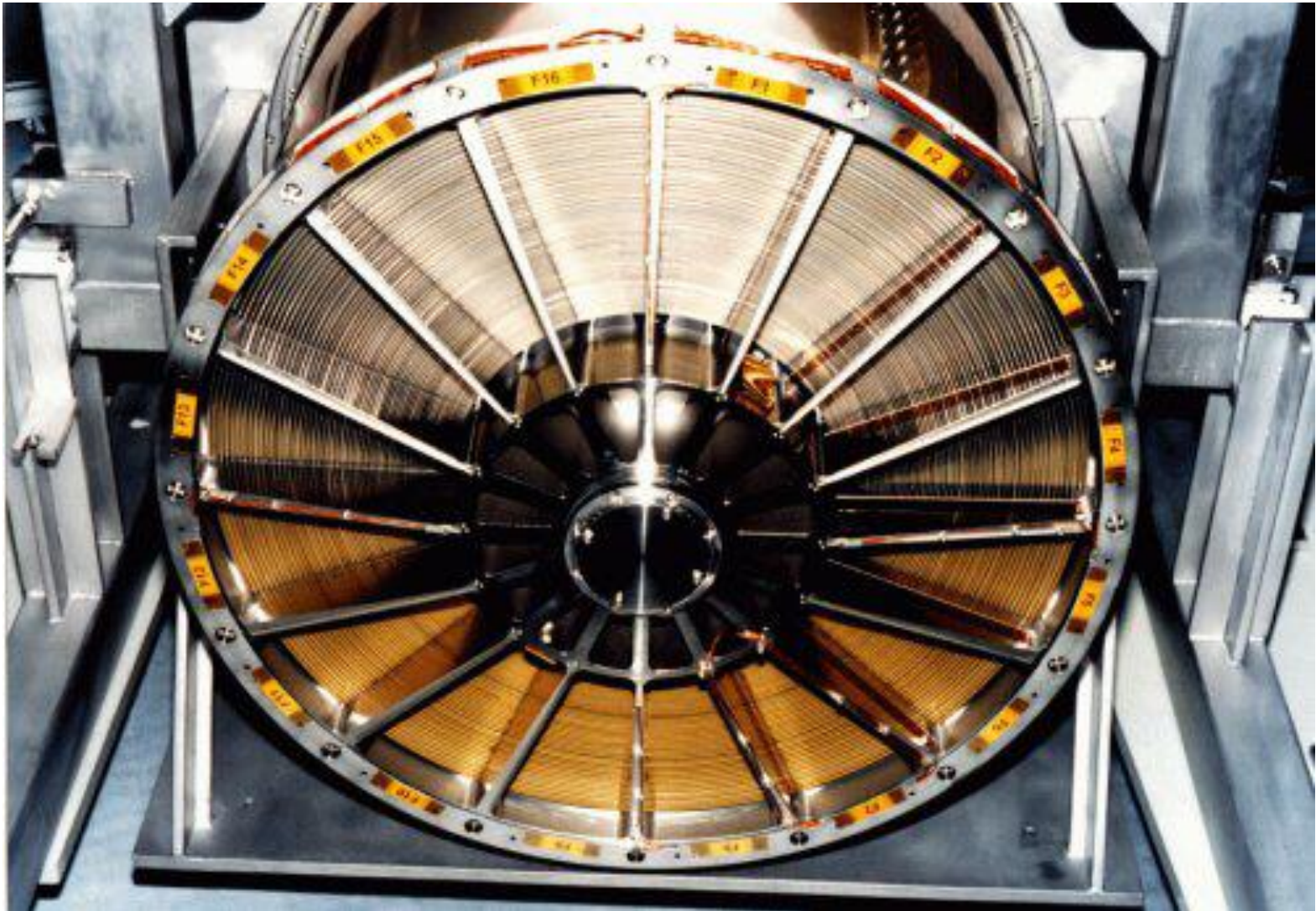
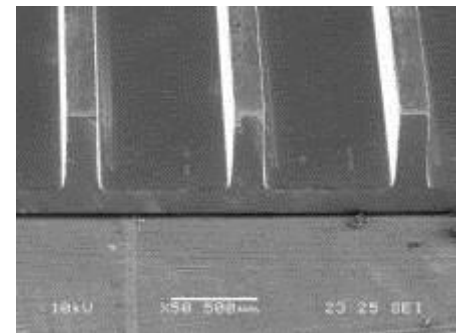
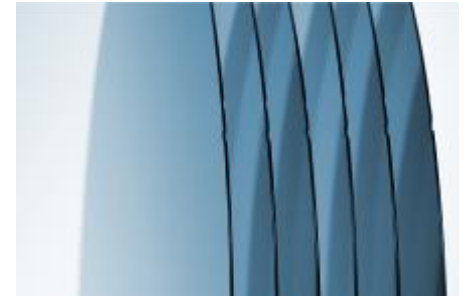
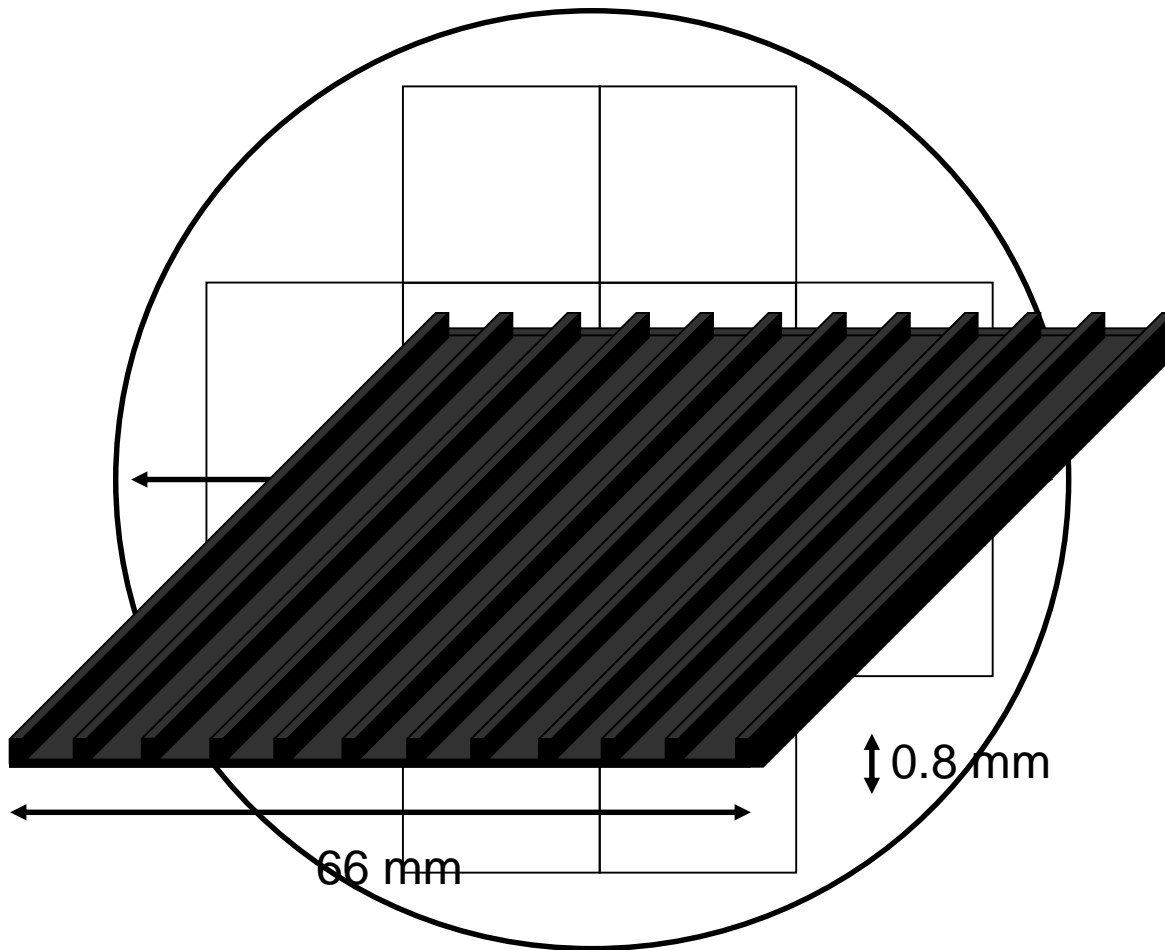


Plate dicing and ribbing

Commercial 300 mm diameter double-sided polished wafer



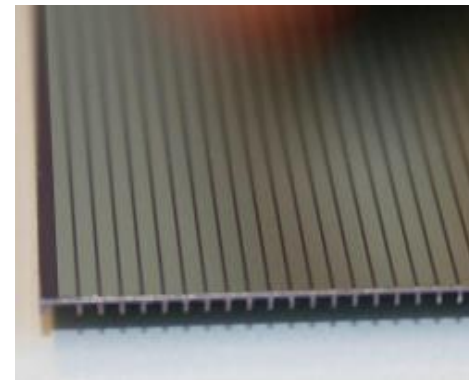
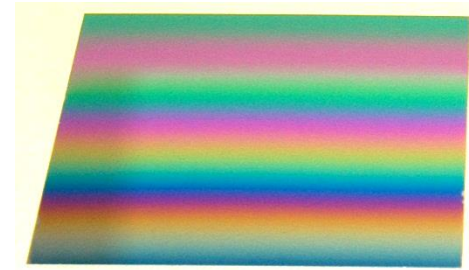
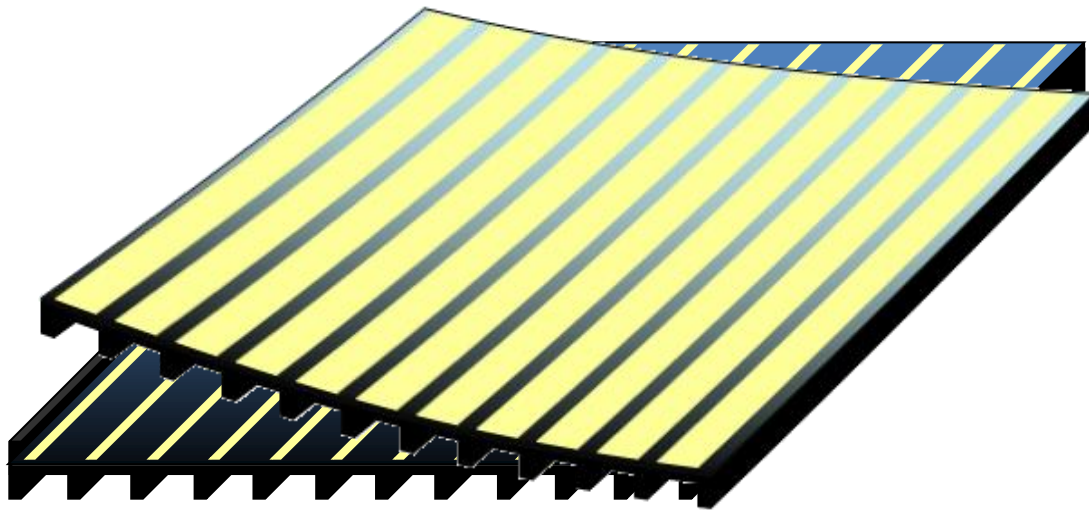


Plate wedging, coating and bending

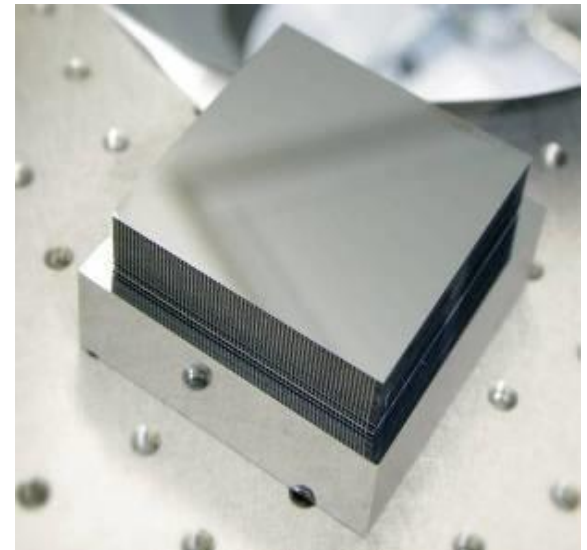
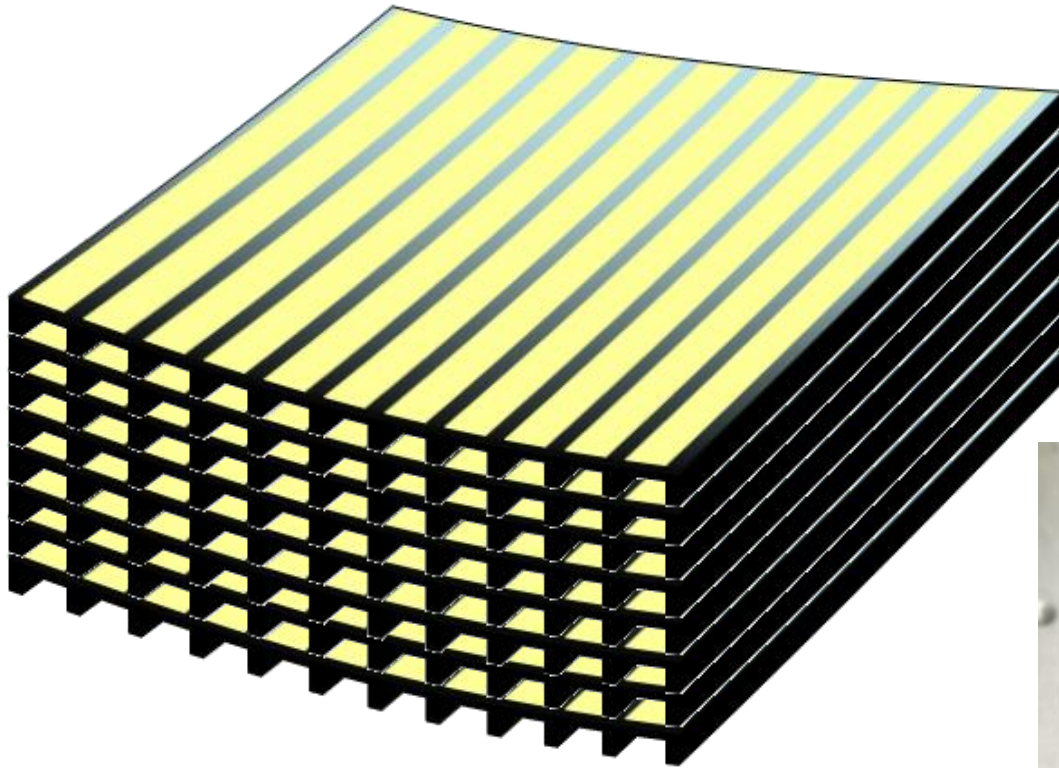
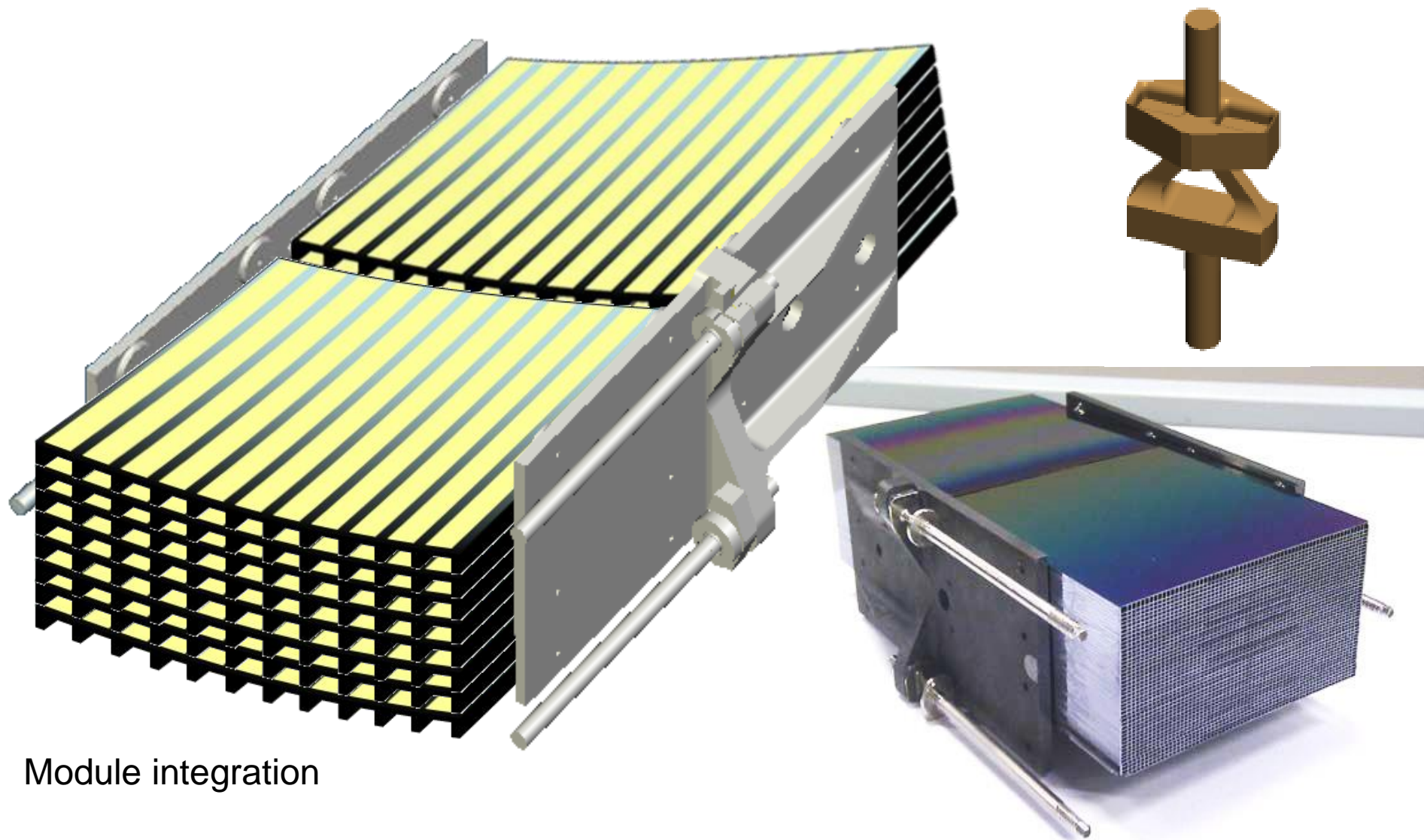
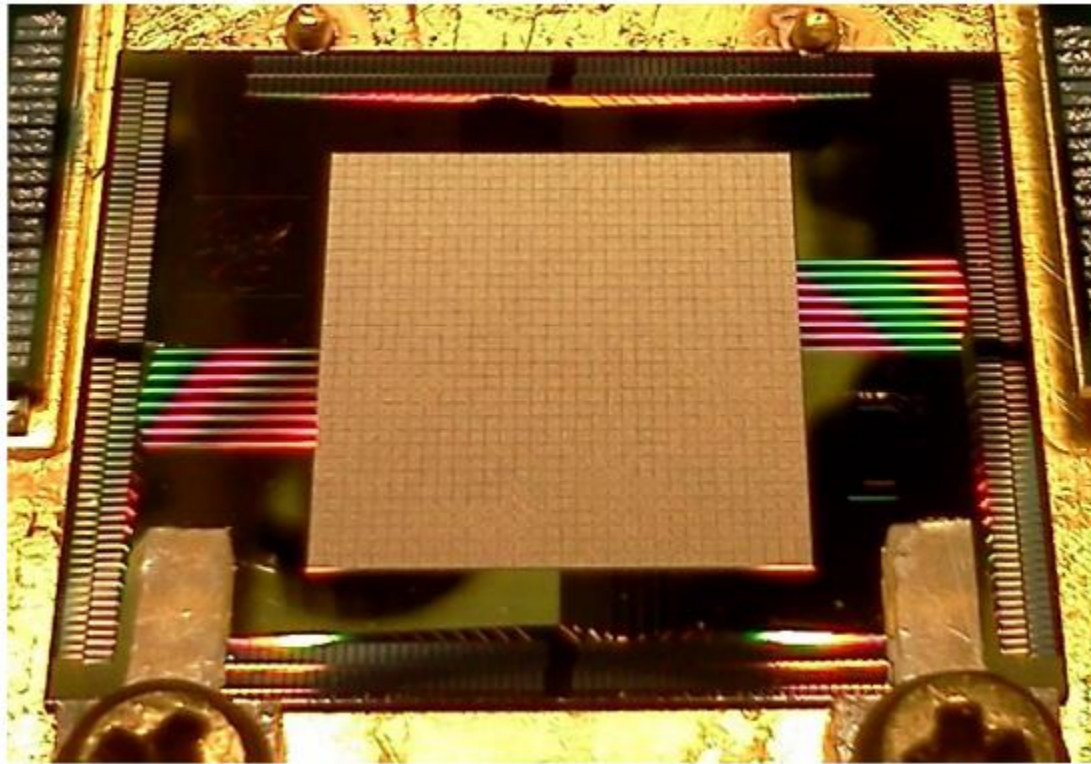


Plate stacking



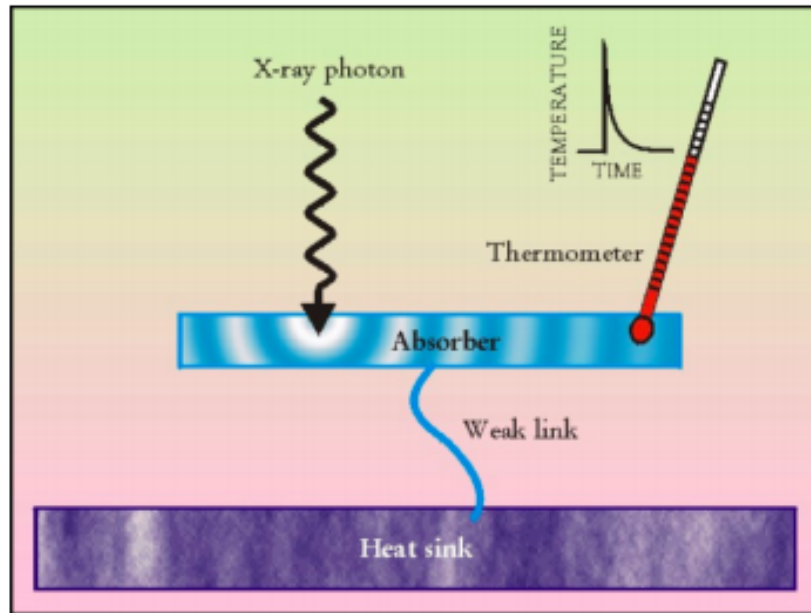
Module integration

X-ray Calorimeter



- 1k pixel array, 300 micron pixel size

Basic Principle

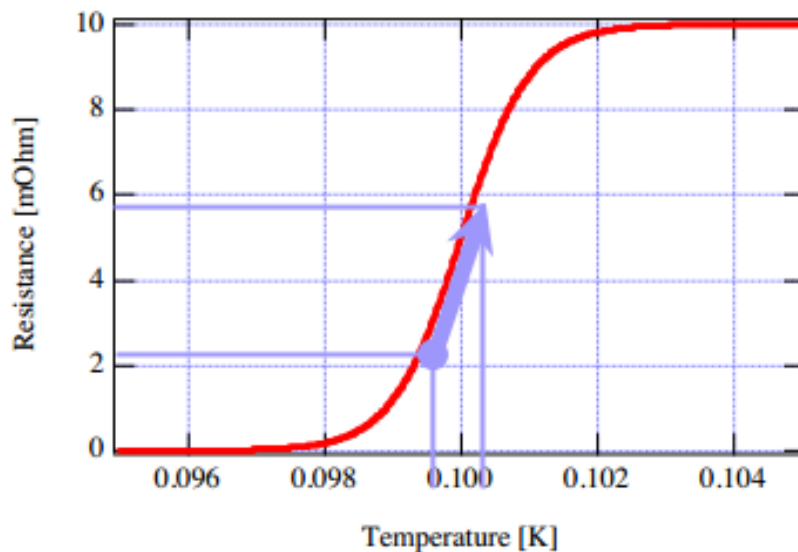


Temperature rise:

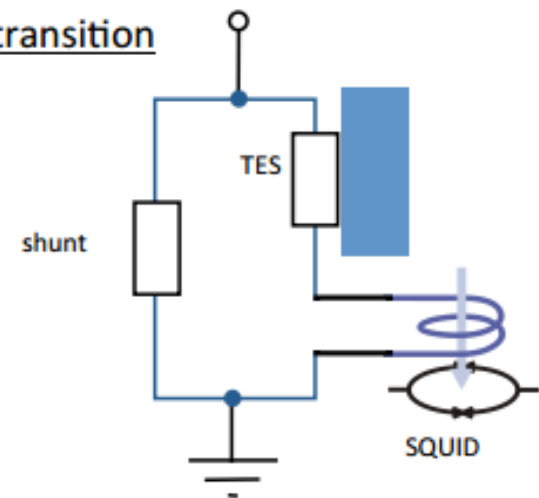
$$\delta T = \frac{E}{C_{\text{tot}}}$$

Energy resolution:

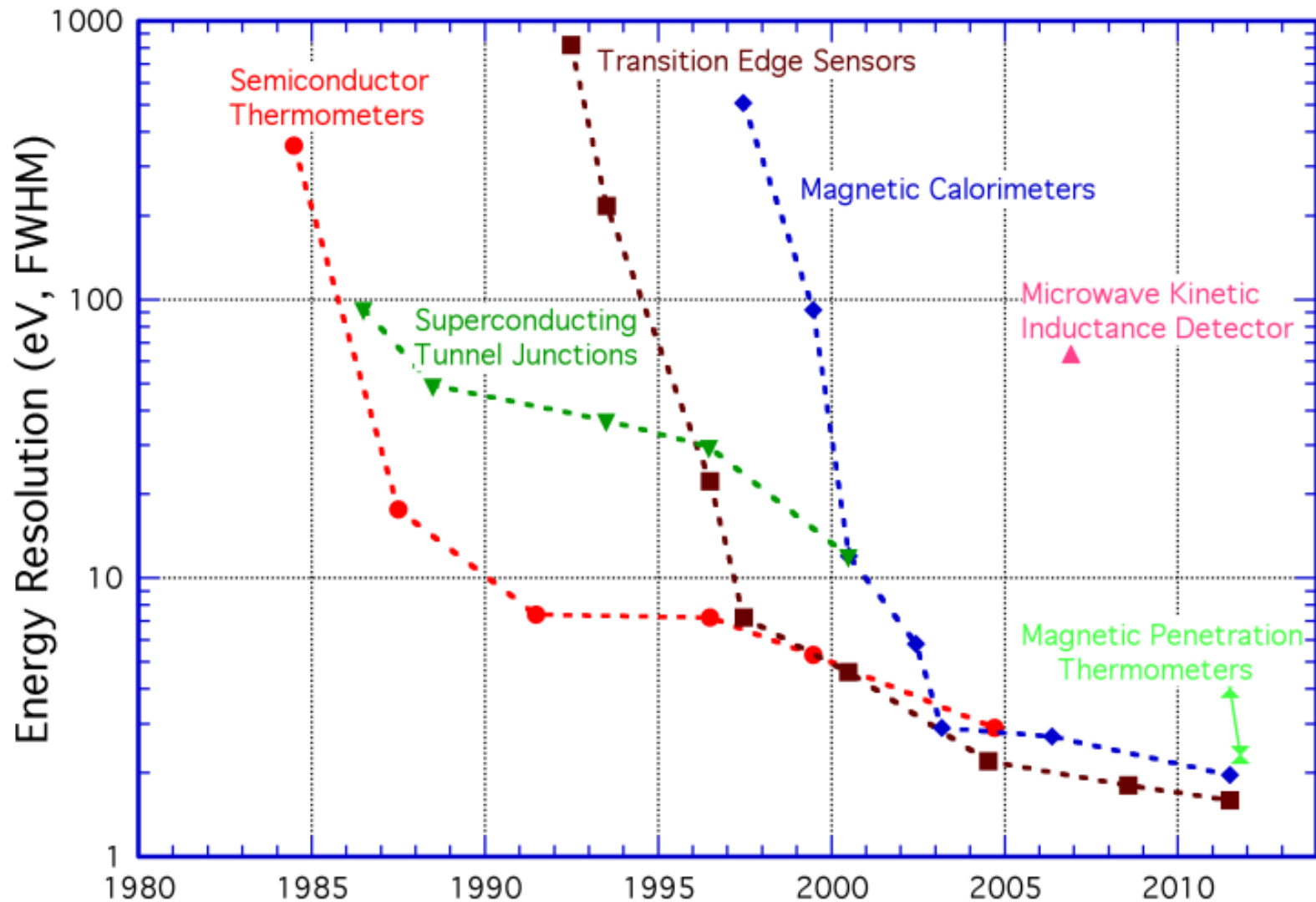
$$\Delta E \sim \sqrt{k_B T^2 C}$$

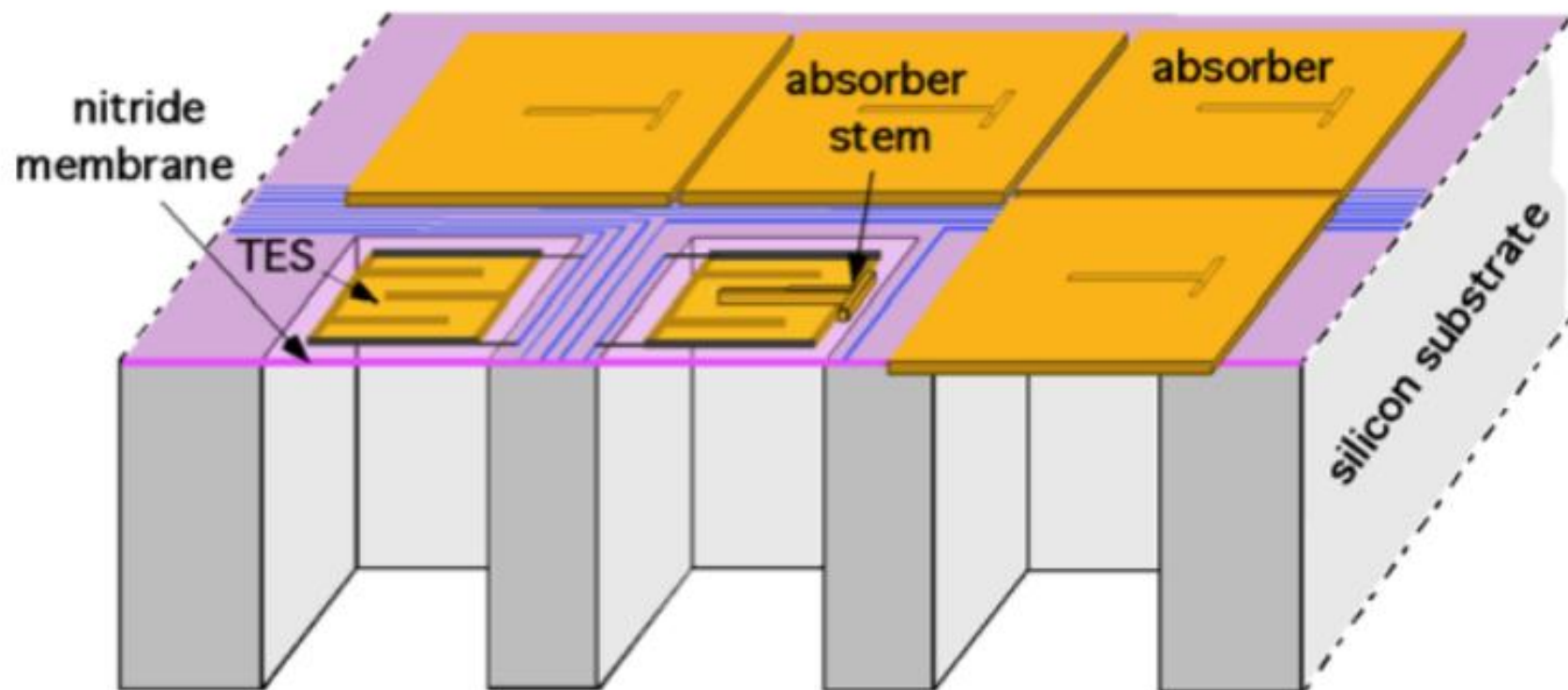


Superconductor voltage-biased
in its transition



Long road towards theoretical performance





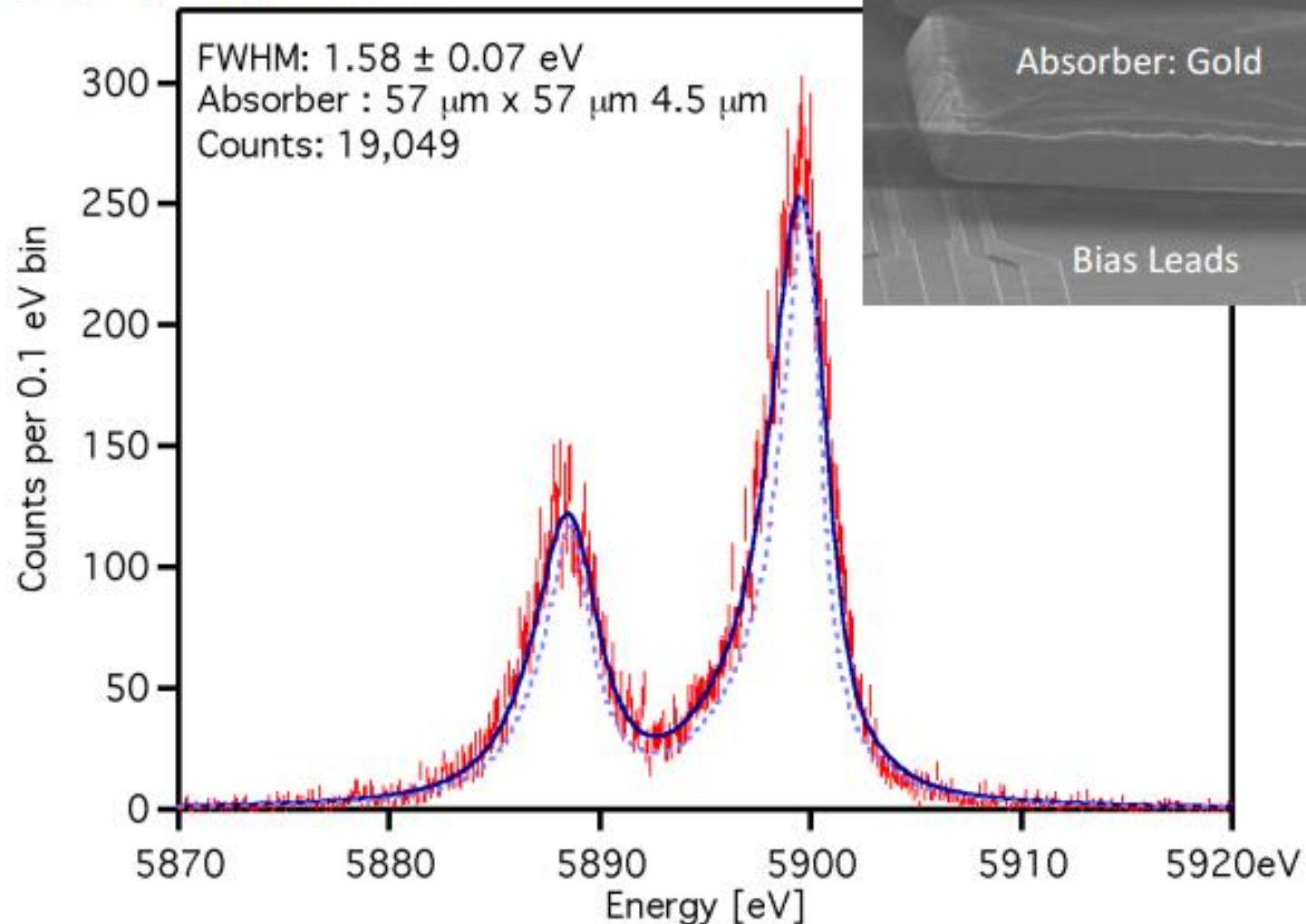
TES: Mo (50 nm) / Au (225 nm)

$T_c \sim 0.1 \text{ K}$

Improving Resolution

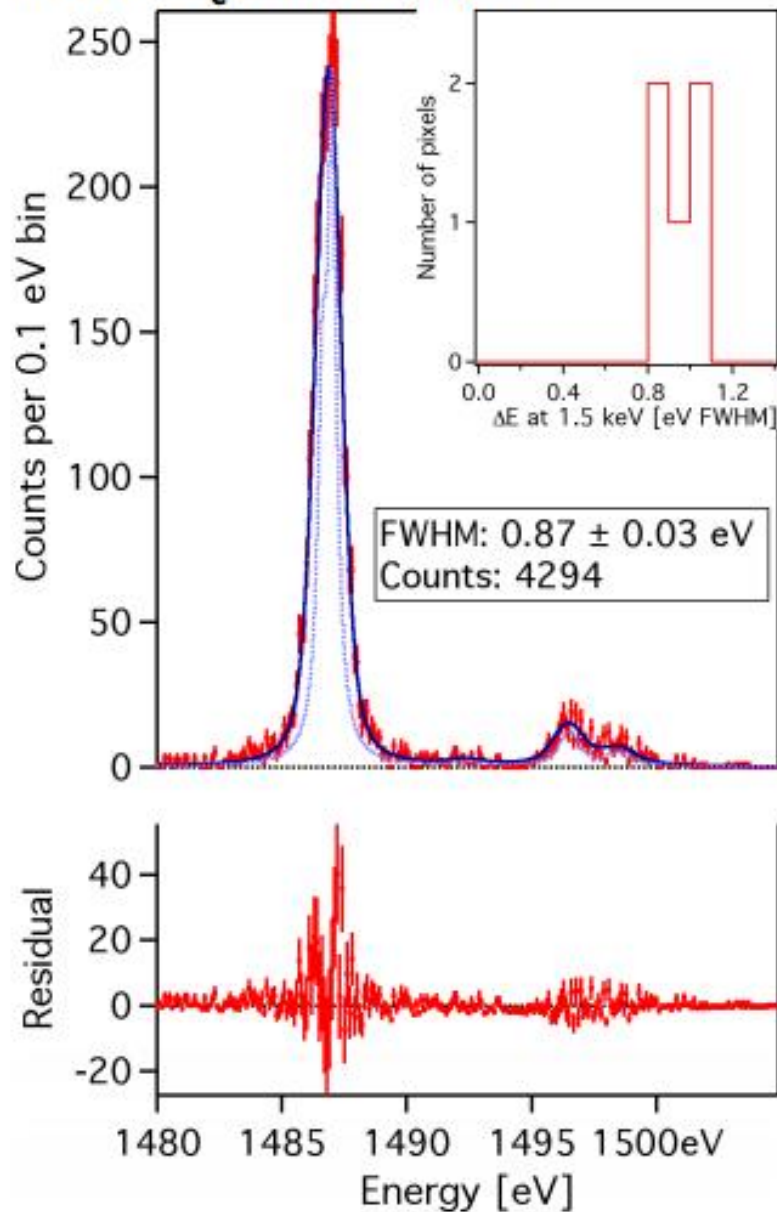
- The physical properties of the superconducting-to-normal transition is fundamental for optimizing the design and performance of TES
- Critical current I_c measurements of square Mo/Au bilayer structures show that they act as weak superconducting links, exhibiting oscillatory behavior with applied magnetic field.
- Measurements show significant departure from similar measurements on simple bilayer test structures.
- This is thought to be due to the presence of additional features (such as noise-mitigation stripes and absorber-attachment stems) introducing spatial inhomogeneity to the superconducting order parameter and current density distribution.
- This is further complicated by the presence of self-induced magnetic fields generated by current flowing in the electrical bias leads and sensor itself.

Higher T_c Small Pixels:



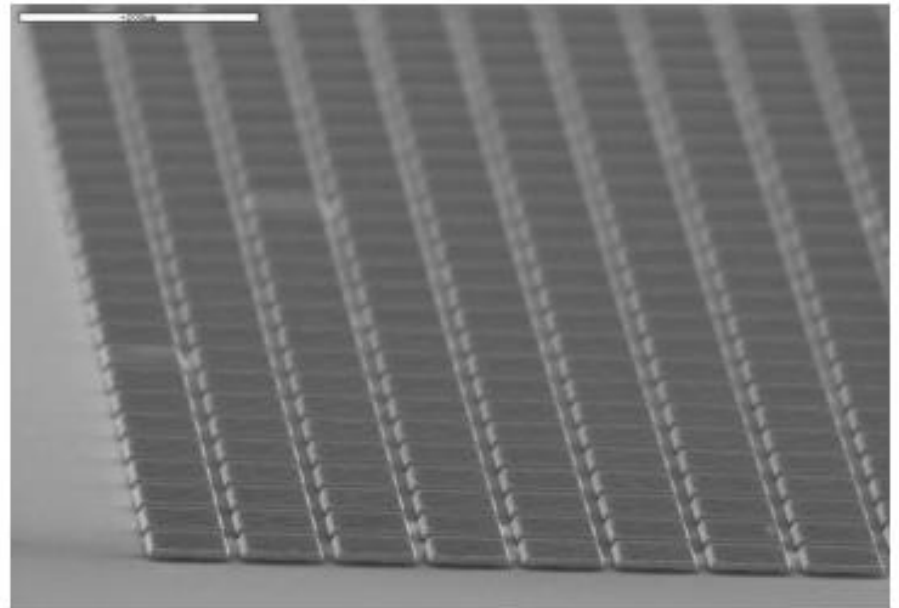
- Best energy resolution detecting 6 keV x-rays with an energy dispersive detector
- High count rate capability
- More demanding read-out requirements

Lower T_c Small Pixels:



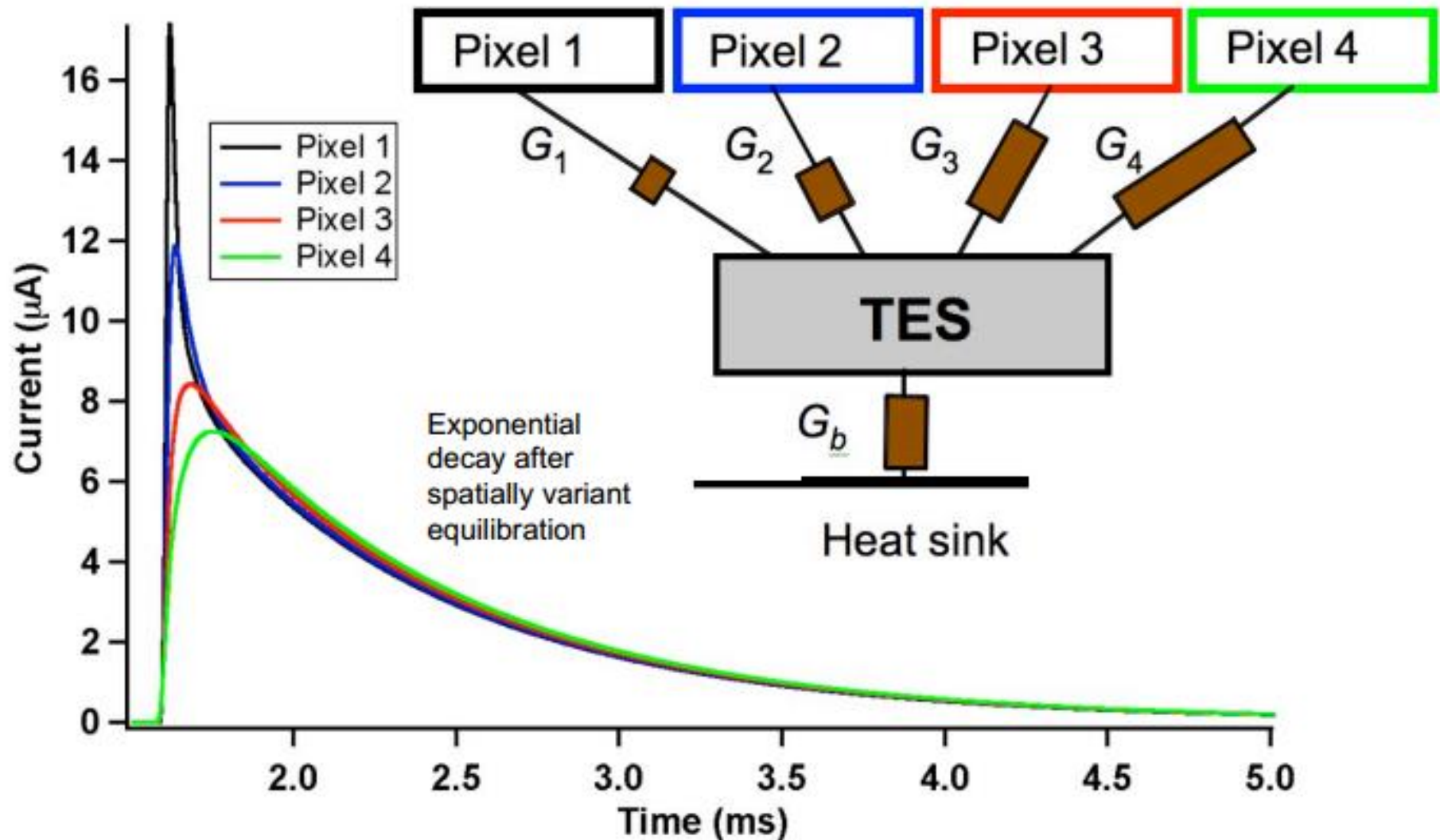
First sub-eV energy resolution result for an X-ray microcalorimeter – at 1.5 keV

- TES on 75 micron pitch
- Absorber: $65\mu\text{m} \times 65\mu\text{m} \times 5.0\mu\text{m}$
- Similar signal speeds / count rate capability to standard pixel design

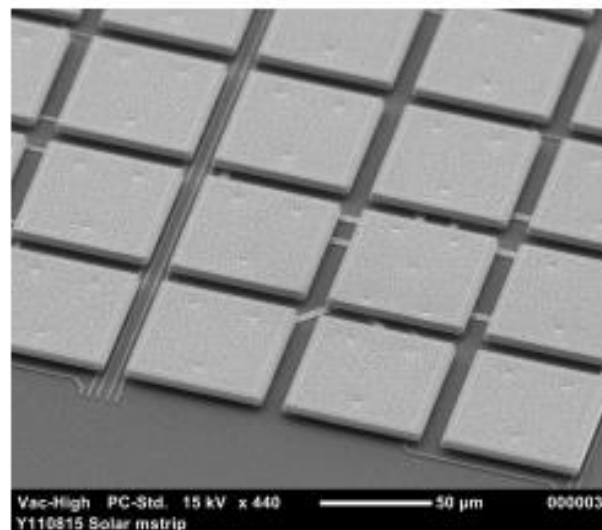
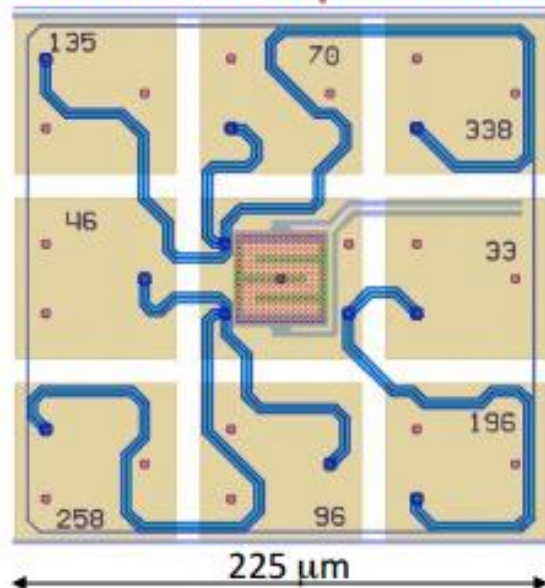


Multi Absorber TES "Hydras" - 1 TES, 4 absorbers

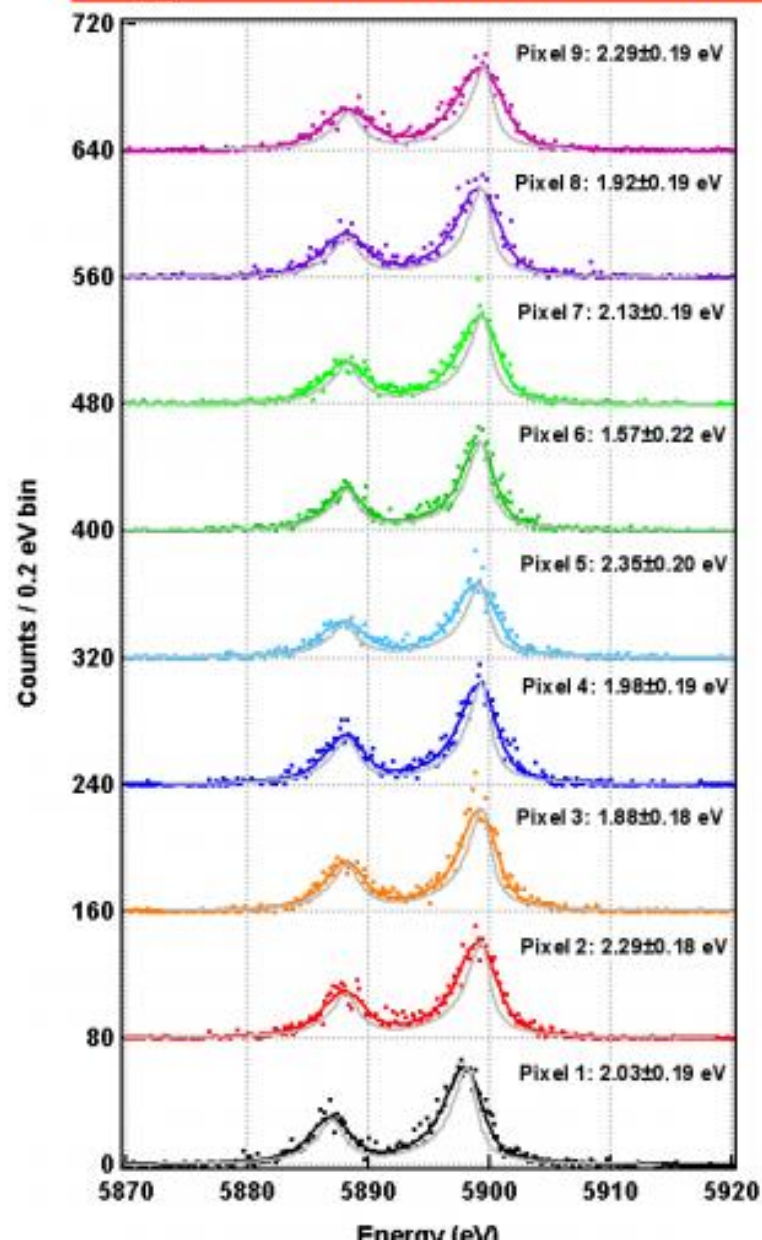
– increase field of view for a fixed number of read-out channels



Hydras with 3x3 array of 65 μm absorbers, 5.0 μm thick

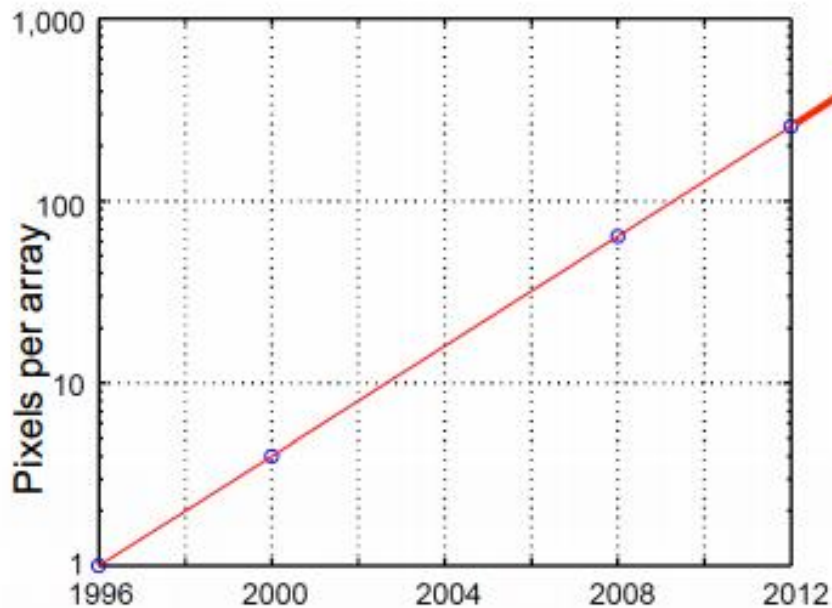
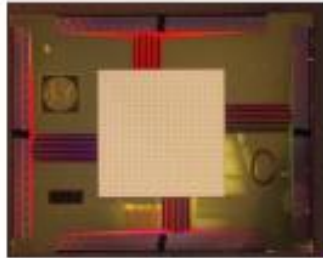


$\Delta E_{\text{rms}} = 2.4 \text{ eV (FWHM)}$ at 6 keV, Mn-K α



Moore's Law

Doubling time: 2 years



1. TES with TDM
2. TES with CDM
3. TES or MCC or MKID with GHz FDM
4. TES or MCC with GHz FDM + CDM



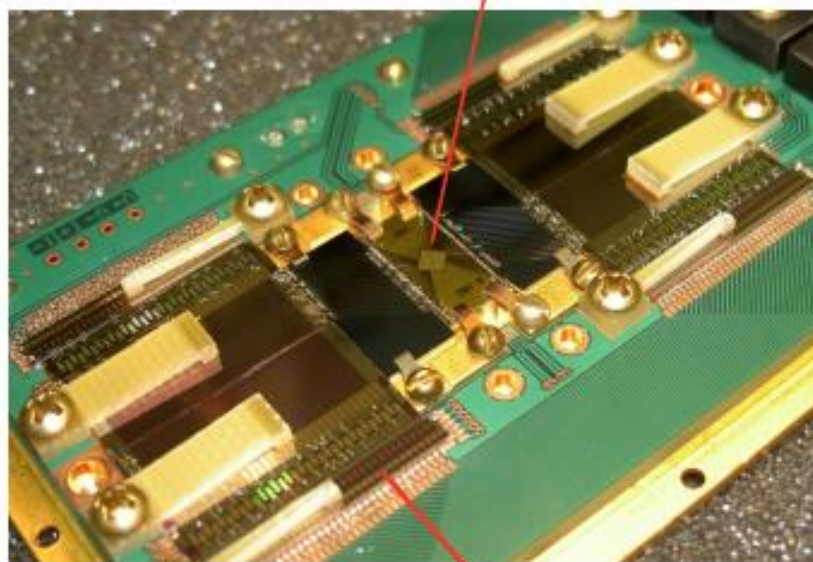
Time Division Multiplexing

GSFC 8 x 8 array
NIST SQUID MUX readout

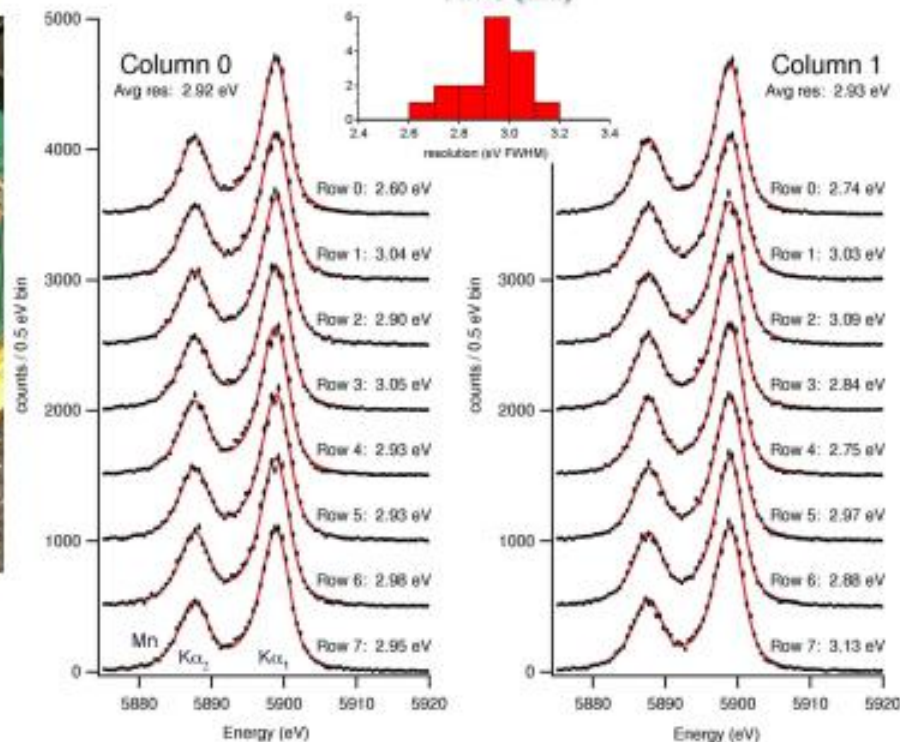
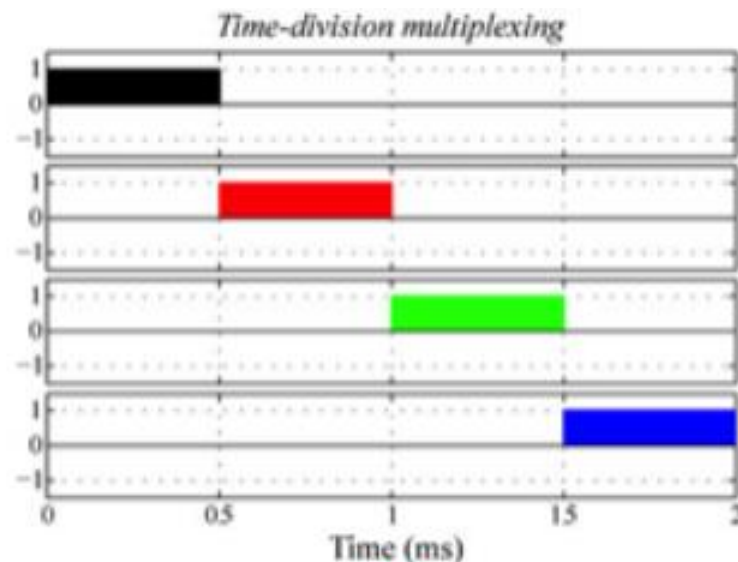
2 x 8 mux readout of 8x8 array

$$\Delta E_{\text{FWHM}} = 2.9 \text{ eV}$$

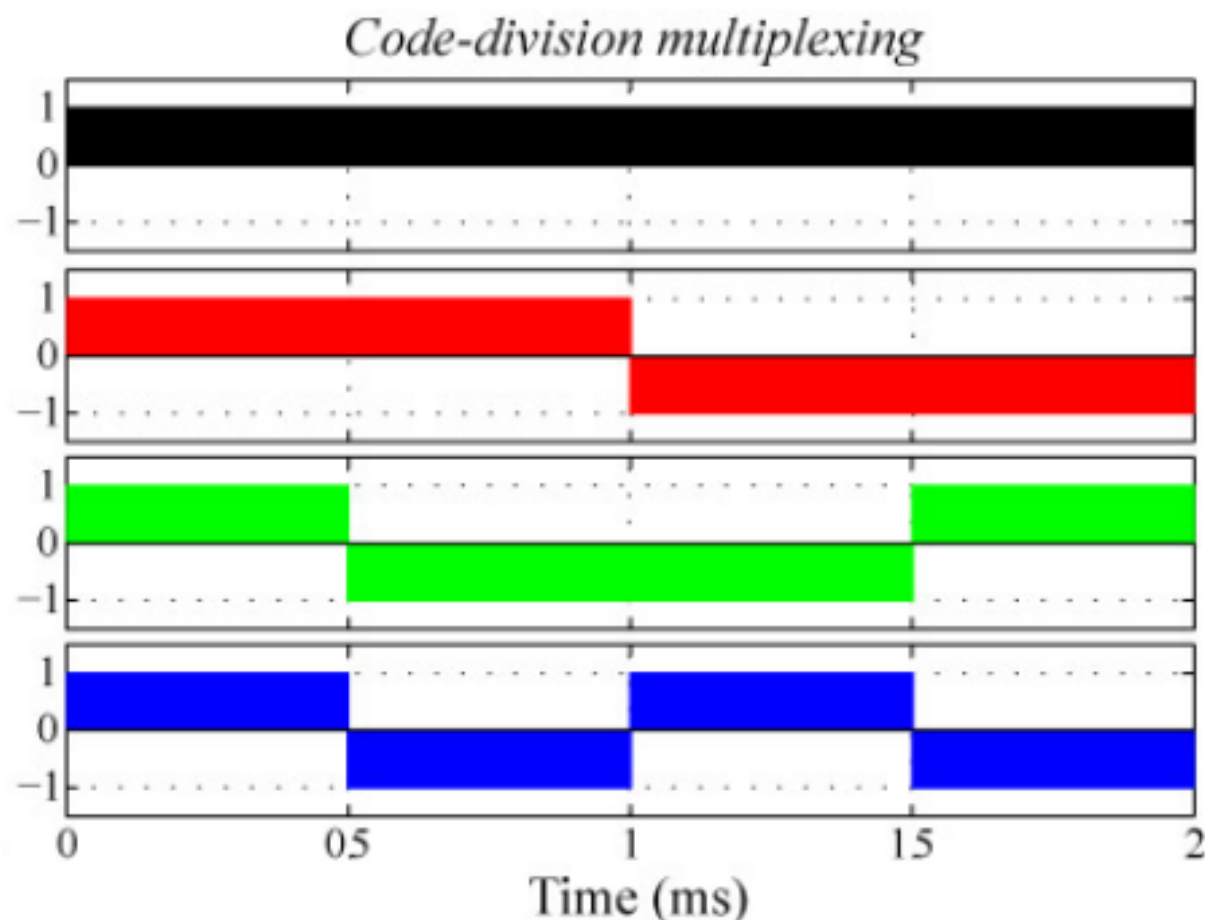
Calorimeter array



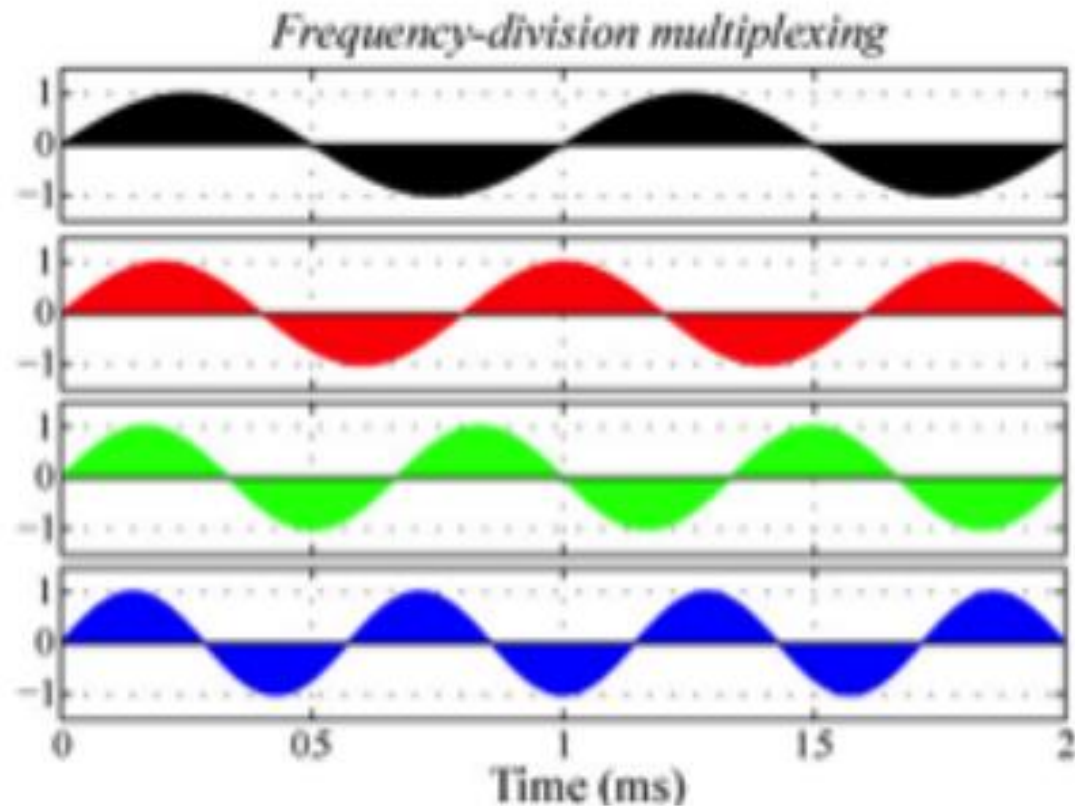
SQUID
multiplexers



CDM: better dynamic range, energy resolution than TDM



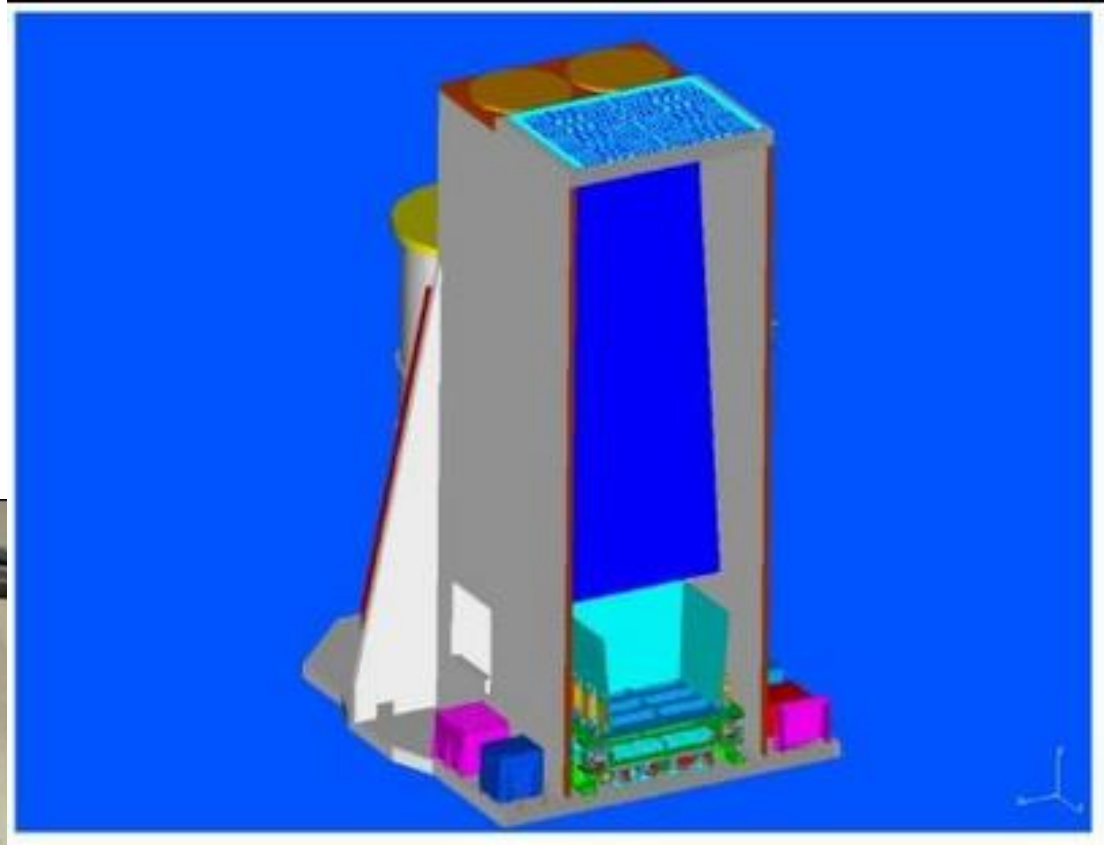
- Every detector pixel is on all of the time
- Does not have “multiplex disadvantage” that exists for TDM multiplexing



TES bias modulation

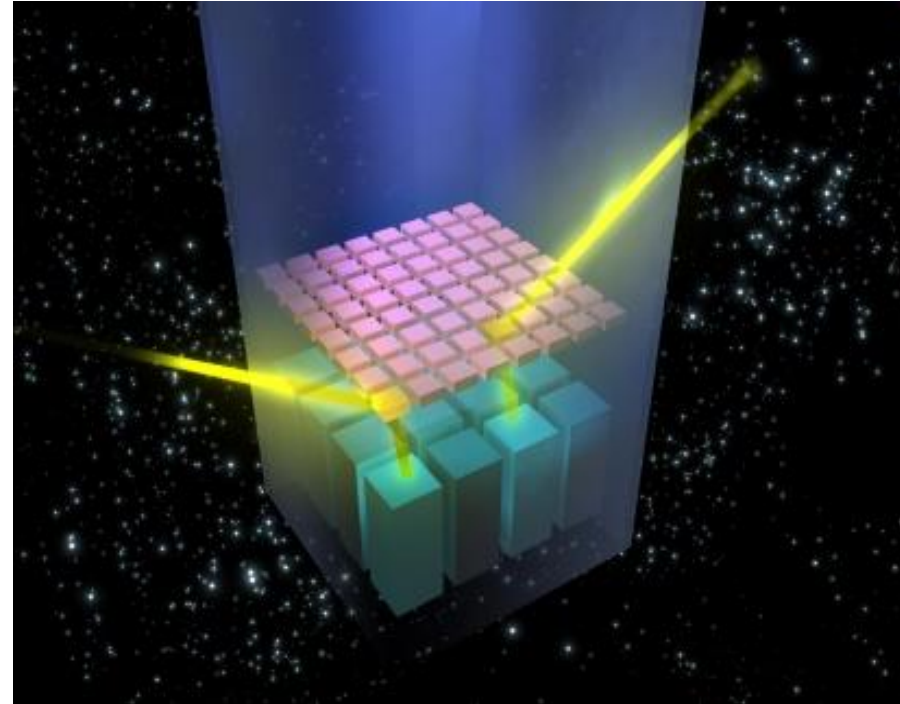
- Different TES pixels AC-biased at different frequencies read out by single amplifier
- X-ray pulses seen in amplitude modulation
- Like CDM, no multiplexing disadvantage

Integral Imager (IBIS)



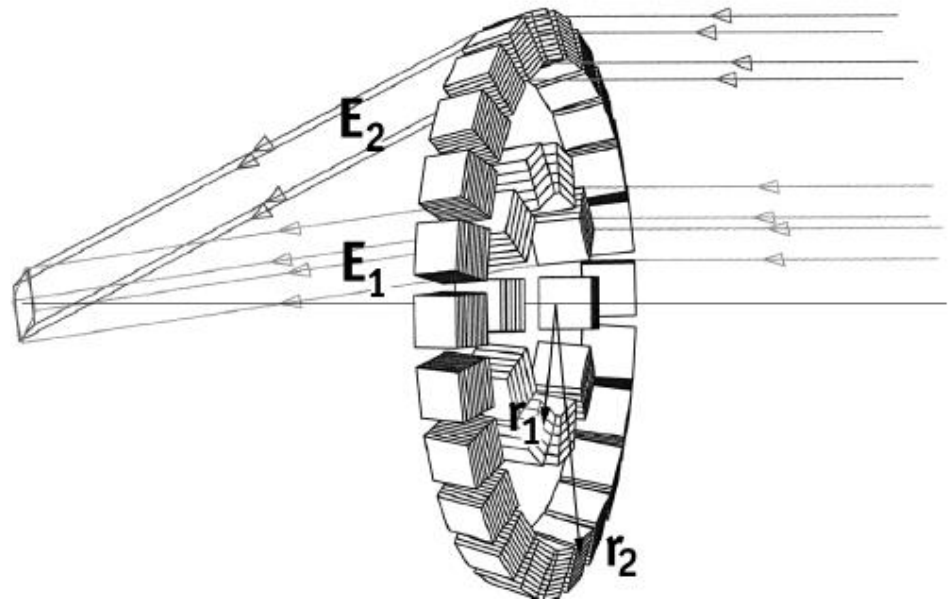
Alternate Imaging Method

- IBIS reconstructs images of powerful events like gamma-ray bursts (GRBs) using radiation passing through the telescope side
- Two detector layers: the higher energy gammas Compton scatter in 1st layer (called ISGRI), losing energy, but not being completely absorbed.
- The deflected (less energetic) rays pass through to lower layer and captured and absorbed The blue-shaded part of the image describes the fully coded field of view of the instrument.



Gamma Ray Focussing

- Coded mask telescopes have only 50% open factor, and detectors must have frontal area equivalent to collecting area
- Large background could be decoupled by focussing advantage – but gamma ray focussing is not easy.



Bragg-relation
 $2 d \sin \theta_B = n \lambda$

Laue Lens

<i>Energy bandpasses</i>	<i>460 – 522 keV</i> <i>825 – 910 keV</i>
<i>Effective area in bandpasses</i>	<i>$\sim 1 \text{ m}^2$</i>
<i>Field of view</i>	<i>$> 30 \text{ arc seconds}$</i>
<i>Angular resolution</i>	<i>$\sim 10 \text{ arc seconds}$</i>
<i>Focal Length</i>	<i>400m</i>

- Rings of Cu and Si crystals for energy bandpass around nuclear emission lines \sim tonnes payload
- Separated telescope and detector spacecraft
- But detector size only $< 10\text{cm}$ – much lower background

Design Issues for Space Astronomy Instruments

- Mass (= M€)
- Power (= large solar arrays = mass)
- Volume (= support structure and mass)
- Radiation (require shielding = mass)
- Cosmic ray removal (processing = mass)
- Calibration (on-ground time and in-orbit efficiency)
- Vacuum (materials, testing time, design effort)
- Thermal (testing, design, power,)
- Thin Filters (single point failure)
- EMC (test on-ground with spacecraft ?)
- Stray light (Baffles, operations = mass / time)
- Pointing (Mechanisms, stability, lifetime)
- Compression (processing=mass, robustness)
- Downlink (Bandwidth = power= mass)